Methods for high-precision determinations of radiative-leptonic decay form factors using lattice QCD

Speaker: Christopher Kane[1]

In collaboration with: Davide Giusti[2], Christoph Lehner[2], Stefan Meinel [1], Amarjit Soni[3]

Jefferson Lab Theory Seminar

Date: September 11, 2023

[1]University of Arizona

[2]University of Regensburg

[3]Brookhaven National Lab

Main Take-Away Points

Main Take-Away Point 1: Radiative leptonic decays are interesting in the regions of small and large photon energies

Main Take-Away Point 2: We have developed methods to achieve high precision for small computational cost

for more details: D. Giusti, **CFK**, C. Lehner, S. Meinel, A. Soni, PRD 2023 / arXiv:[2302.01298]

Main Take-Away Point 3: Working on physical calculation of $D_s \to \gamma \ell \nu_\ell$, out soon

Table of Contents

Outline for section 1

Radiative leptonic decays of pseudoscalar mesons

Flavor changing charged current (FCCC)

- $H^+ \to \gamma \ell^+ \nu_\ell, \quad H^- \to \gamma \ell^- \bar{\nu}_\ell$

Schematic diagram for $D_s^+ \to \gamma e^+ \nu_e$

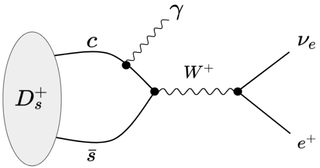

Radiative leptonic decays of pseudoscalar mesons

Flavor changing charged current (FCCC)

- $H^+ \to \gamma \ell^+ \nu_\ell, \quad H^- \to \gamma \ell^- \bar{\nu}_\ell$

Schematic diagram for $D_s^+ \to \gamma e^+ \nu_e$

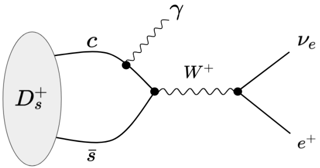

Flavor changing neutral current (FCNC)

- $H^0 \to \gamma \ell^+ \ell^-$

Schematic diagram for $B_s^0 \to \gamma \ell^+ \ell^-$

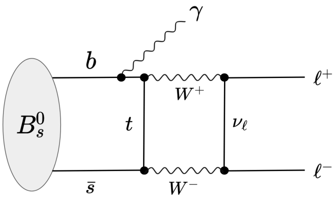

Radiative leptonic decays of pseudoscalar mesons

Flavor changing charged current (FCCC)

- $H^+ \to \gamma \ell^+ \nu_\ell, \quad H^- \to \gamma \ell^- \bar{\nu}_\ell$

Flavor changing neutral current (FCNC)

- $H^0 \to \gamma \ell^+ \ell^-$

Schematic diagram for $D_s^+ \to \gamma e^+ \nu_e$

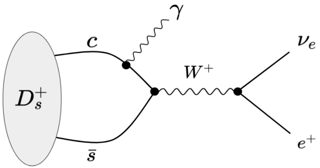

Schematic diagram for $B_s^0 \to \gamma \ell^+ \ell^-$

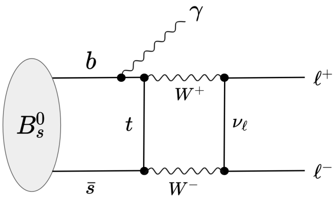

Knowledge of **structure dependent** QCD form factors are of interest for both small and large photon energies

Regions of small photon energies

Precision determinations of CKM matrix elements

Determinations of CKM matrix elements $V_{q_1 q_2}$ require meson decay constants f_H

$$\Gamma(H \to \ell\nu) = \frac{G_F^2}{8\pi}|V_{q_1 q_2}|^2 m_\ell^2 \left(1 - \frac{m_\ell^2}{m_H^2}\right)^2 m_H {f_H}^2, \qquad \langle 0|A_\mu|H\rangle = i p_\mu f_H$$

Precision determinations of CKM matrix elements

Determinations of CKM matrix elements $V_{q_1 q_2}$ require meson decay constants f_H

$$\Gamma(H \to \ell\nu) = \frac{G_F^2}{8\pi}|V_{q_1 q_2}|^2 m_\ell^2 \left(1 - \frac{m_\ell^2}{m_H^2}\right)^2 m_H {f_H}^2, \qquad \langle 0|A_\mu|H\rangle = ip_\mu f_H$$

$$\left.\begin{array}{l}\text{Measure } \Gamma(H \to \ell\nu) \text{ experimentally} \\ \text{Calculate } f_H \text{ with lattice QCD}\end{array}\right\} \text{ determine } |V_{q_1 q_2}|^2$$

Precision determinations of CKM matrix elements

Determinations of CKM matrix elements $V_{q_1 q_2}$ require meson decay constants f_H

$$\Gamma(H \to \ell\nu) = \frac{G_F^2}{8\pi}|V_{q_1 q_2}|^2 m_\ell^2 \left(1 - \frac{m_\ell^2}{m_H^2}\right)^2 m_H {f_H}^2, \qquad \langle 0|A_\mu|H\rangle = i p_\mu f_H$$

$$\left.\begin{array}{l}\text{Measure } \Gamma(H \to \ell\nu) \text{ experimentally} \\ \text{Calculate } f_H \text{ with lattice QCD}\end{array}\right\} \text{ determine } |V_{q_1 q_2}|^2$$

- Sub-percent precision for f_H require $\mathcal{O}(\alpha_{em})$ electromagnetic corrections $H \to \ell\nu(\gamma)$
- Radiative leptonic decay rate $H \to \gamma\ell\nu$ required to subtract IR divergences in $H \to \ell\nu(\gamma)$ $\to$ by the Bloch-Nordsieck mechanism [Bloch, Nordsieck, PRD 1937]

Precision determinations of CKM matrix elements

Determinations of CKM matrix elements $V_{q_1 q_2}$ require meson decay constants f_H

$$\Gamma(H \to \ell\nu) = \frac{G_F^2}{8\pi} |V_{q_1 q_2}|^2 m_\ell^2 \left(1 - \frac{m_\ell^2}{m_H^2}\right)^2 m_H {f_H}^2, \qquad \langle 0|A_\mu|H\rangle = i p_\mu f_H$$

$$\left.\begin{array}{l}\text{Measure } \Gamma(H \to \ell\nu) \text{ experimentally} \\ \text{Calculate } f_H \text{ with lattice QCD}\end{array}\right\} \text{ determine } |V_{q_1 q_2}|^2$$

- Sub-percent precision for f_H require $\mathcal{O}(\alpha_{em})$ electromagnetic corrections $H \to \ell\nu(\gamma)$
- Radiative leptonic decay rate $H \to \gamma\ell\nu$ required to subtract IR divergences in $H \to \ell\nu(\gamma)$ $\to$ by the Bloch-Nordsieck mechanism [Bloch, Nordsieck, PRD 1937]

Approx. π^-, K^- as point-like

- $\pi^- \to \mu^-\bar{\nu}_\mu\gamma$ and $K^- \to \mu^-\bar{\nu}_\mu\gamma$

[N. Carrasco et. al, PRD 2015 / arXiv:1502.00257]

Precision determinations of CKM matrix elements

Determinations of CKM matrix elements $V_{q_1 q_2}$ require meson decay constants f_H

$$\Gamma(H \to \ell\nu) = \frac{G_F^2}{8\pi}|V_{q_1 q_2}|^2 m_\ell^2 \left(1 - \frac{m_\ell^2}{m_H^2}\right)^2 m_H {f_H}^2, \qquad \langle 0|A_\mu|H\rangle = i p_\mu f_H$$

$$\left.\begin{array}{l}\text{Measure } \Gamma(H \to \ell\nu) \text{ experimentally} \\ \text{Calculate } f_H \text{ with lattice QCD}\end{array}\right\} \text{ determine } |V_{q_1 q_2}|^2$$

- Sub-percent precision for f_H require $\mathcal{O}(\alpha_{em})$ electromagnetic corrections $H \to \ell\nu(\gamma)$
- Radiative leptonic decay rate $H \to \gamma\ell\nu$ required to subtract IR divergences in $H \to \ell\nu(\gamma)$ $\to$ by the Bloch-Nordsieck mechanism [Bloch, Nordsieck, PRD 1937]

Approx. π^-, K^- as point-like

- $\pi^- \to \mu^-\bar{\nu}_\mu\gamma$ and $K^- \to \mu^-\bar{\nu}_\mu\gamma$

Structure dependent form factors required

- $\pi^- \to e^-\bar{\nu}_e\gamma$ and $K^- \to e^-\bar{\nu}_e\gamma$

[N. Carrasco et. al, PRD 2015 / arXiv:1502.00257]

Regions of large photon energies

FCNC processes $B_s^0 \to \ell^+\ell^-\gamma$ and $B^0 \to \ell^+\ell^-\gamma$

$B_s^0 \sim \bar{b}\, s$
$B^0 \sim \bar{b}\, d$

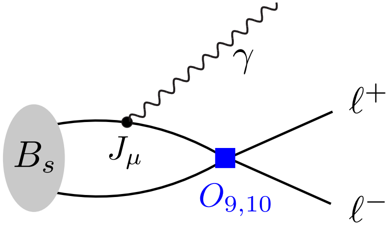

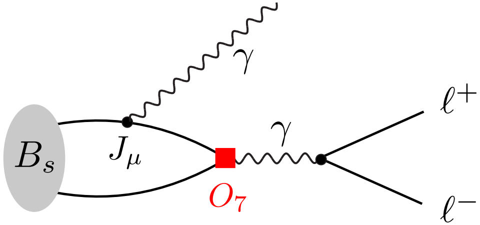

- Hard photon removes helicity suppression $(m_\ell/m_B)^2$
- This process sensitive to all operators in the $b \to s\ell^+\ell^-$ weak effective Hamiltonian including O_9, where slight tension with SM prediction exists

  [Greljo, Salko, Smolkovic, Stangl, JHEP 2023 / arXiv:2212.10497]

FCNC processes $B_s^0 \to \ell^+\ell^-\gamma$ and $B^0 \to \ell^+\ell^-\gamma$

$B_s^0 \sim \bar{b}\, s$
$B^0 \sim \bar{b}\, d$

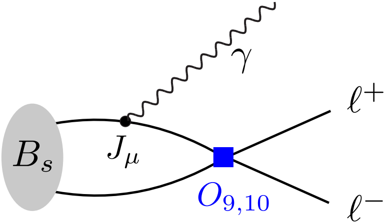

- Hard photon removes helicity suppression $(m_\ell/m_B)^2$
- This process sensitive to all operators in the $b \to s\ell^+\ell^-$ weak effective Hamiltonian including O_9, where slight tension with SM prediction exists

  [Greljo, Salko, Smolkovic, Stangl, JHEP 2023 / arXiv:2212.10497]

- $\mathcal{B}(B^0 \to \ell^+\ell^-\gamma) < \mathcal{O}(10^{-7})$ for $\ell = e, \mu$ [BABAR: PRD 2008 / arXiv:0706.2870]
- $\mathcal{B}(B_s^0 \to \mu^+\mu^-\gamma) < 2.0 \times 10^{-9}$ for $m_{\mu\mu} > 4.9$ GeV [LHCb: PRD 2022 / arXiv:2108.09283]

FCCC process $B^- \to \gamma \ell^- \bar{\nu}$

$B^- \sim b\,\bar{u}$

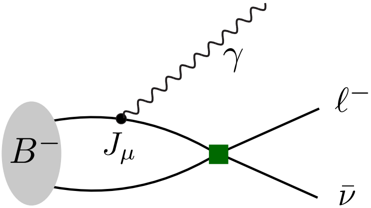

- Hard photon removes helicity suppression $(m_\ell/m_B)^2$
- For large $E_\gamma^{(0)}$, simplest decay that probes the inverse moment of the B meson lightcone distribution amplitude

$$\frac{1}{\lambda_B} = \int_0^\infty d\omega \; \frac{\Phi_{B+}(\omega)}{\omega}$$

- λ_B important input in QCD factorization approach to exclusive B decays, currently not well known
  [See e.g., Beneke, Braun, Ji, Wei, arXiv:1804.04962/JHEP 2018;

  Beneke, Buchalla, Neubert, Sachrajda, arXiv:hep-ph/9905312/PRL 1999]

FCCC process $B^- \to \gamma \ell^- \bar{\nu}$

$B^- \sim b\,\bar{u}$

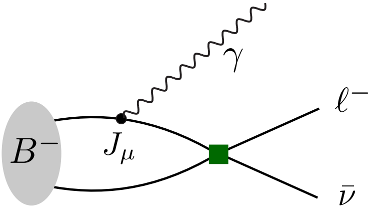

- Hard photon removes helicity suppression $(m_\ell/m_B)^2$
- For large $E_\gamma^{(0)}$, simplest decay that probes the inverse moment of the B meson lightcone distribution amplitude

$$\frac{1}{\lambda_B} = \int_0^\infty d\omega\, \frac{\Phi_{B+}(\omega)}{\omega}$$

- λ_B important input in QCD factorization approach to exclusive B decays, currently not well known
  [See e.g., Beneke, Braun, Ji, Wei, arXiv:1804.04962/JHEP 2018;

  Beneke, Buchalla, Neubert, Sachrajda, arXiv:hep-ph/9905312/PRL 1999]
- Belle: $\mathcal{B}(B^+ \to \ell^+ \nu \gamma) < 3.0 \times 10^{-6}$ $(E_\gamma^{(0)} > 1$ GeV$)$ [arXiv:1810.12976/PRD 2018]

Experimental status of radiative leptonic decays

- $K^- \to e^-\bar{\nu}\gamma$, $K^- \to \mu^-\bar{\nu}\gamma$, $\pi^- \to e^-\bar{\nu}\gamma$, $\pi^- \to \mu^-\bar{\nu}\gamma$
  $\to K^-, \pi^-$ partial branching fractions, photon-energy spectra, and angular distributions known from multiple experiments. [See PDG review by M. Bychkov and G. D'Ambrosio, 2018]

Experimental status of radiative leptonic decays

- $K^- \to e^- \bar{\nu}\gamma$, $K^- \to \mu^- \bar{\nu}\gamma$, $\pi^- \to e^- \bar{\nu}\gamma$, $\pi^- \to \mu^- \bar{\nu}\gamma$
  $\to K^-, \pi^-$ partial branching fractions, photon-energy spectra, and angular distributions known from multiple experiments. [See PDG review by M. Bychkov and G. D'Ambrosio, 2018]

- $D_s^+ \to e^+ \nu\gamma$: $\mathcal{B}(E_\gamma^{(0)} > 10\text{ MeV }) < 1.3 \times 10^{-4}$ [BESIII: PRD 2017 / arXiv:1702.05837]
- $D^+ \to e^+ \nu\gamma$: $\mathcal{B}(E_\gamma^{(0)} > 10\text{ MeV }) < 3.0 \times 10^{-5}$ [BESIII: PRD 2019 / arXiv:1902.03351]

Experimental status of radiative leptonic decays

- $K^- \to e^-\bar{\nu}\gamma$, $K^- \to \mu^-\bar{\nu}\gamma$, $\pi^- \to e^-\bar{\nu}\gamma$, $\pi^- \to \mu^-\bar{\nu}\gamma$
$\to K^-, \pi^-$ partial branching fractions, photon-energy spectra, and angular distributions known from multiple experiments. [See PDG review by M. Bychkov and G. D'Ambrosio, 2018]

- $D_s^+ \to e^+\nu\gamma$: $\mathcal{B}(E_\gamma^{(0)} > 10 \text{ MeV }) < 1.3 \times 10^{-4}$ [BESIII: PRD 2017 / arXiv:1702.05837]
- $D^+ \to e^+\nu\gamma$: $\mathcal{B}(E_\gamma^{(0)} > 10 \text{ MeV }) < 3.0 \times 10^{-5}$ [BESIII: PRD 2019 / arXiv:1902.03351]

- $\mathcal{B}(B^+ \to \ell^+\nu\gamma) < 3.0 \times 10^{-6}$ $(E_\gamma^{(0)} > 1 \text{ GeV})$ [Belle: PRD 2018 / arXiv:1810.12976]
- Belle II expected to measure $\mathcal{B}(B^+ \to \ell^+\nu\gamma)$ with 3.6% statistical uncertainty
[Belle: PRD 2018 / arXiv:1810.12976]

Experimental status of radiative leptonic decays

- $K^- \to e^- \bar{\nu}\gamma$, $K^- \to \mu^- \bar{\nu}\gamma$, $\pi^- \to e^- \bar{\nu}\gamma$, $\pi^- \to \mu^- \bar{\nu}\gamma$
  $\to K^-, \pi^-$ partial branching fractions, photon-energy spectra, and angular distributions known from multiple experiments. [See PDG review by M. Bychkov and G. D'Ambrosio, 2018]

- $D_s^+ \to e^+\nu\gamma$: $\mathcal{B}(E_\gamma^{(0)} > 10$ MeV $) < 1.3 \times 10^{-4}$ [BESIII: PRD 2017 / arXiv:1702.05837]
- $D^+ \to e^+\nu\gamma$: $\mathcal{B}(E_\gamma^{(0)} > 10$ MeV $) < 3.0 \times 10^{-5}$ [BESIII: PRD 2019 / arXiv:1902.03351]

- $\mathcal{B}(B^+ \to \ell^+\nu\gamma) < 3.0 \times 10^{-6}$ $(E_\gamma^{(0)} > 1$ GeV$)$ [Belle: PRD 2018 / arXiv:1810.12976]
- Belle II expected to measure $\mathcal{B}(B^+ \to \ell^+\nu\gamma)$ with 3.6% statistical uncertainty [Belle: PRD 2018 / arXiv:1810.12976]
- $\mathcal{B}(B^0 \to \ell^+\ell^-\gamma) < \mathcal{O}(10^{-7})$ for $\ell = e, \mu$ [BABAR: PRD 2008 / arXiv:0706.2870]
- $\mathcal{B}(B_s^0 \to \mu^+\mu^-\gamma) < 2.0 \times 10^{-9}$ for $m_{\mu\mu} > 4.9$ GeV [LHCb: PRD 2022 / arXiv:2108.09283]

Review of lattice calculations of radiative leptonic decays

Lattice 2019
present first results

CFK, et. al, [arXiv:1907.00279]

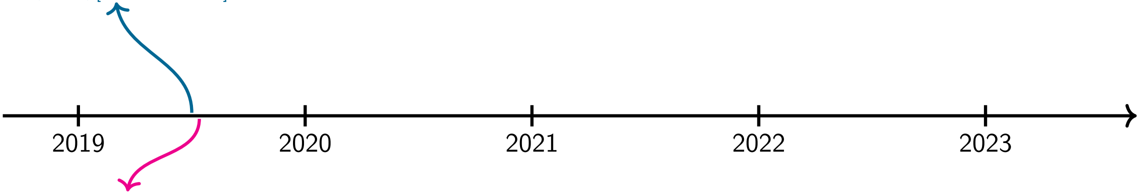

Lattice 2019
present first results

G. Martinelli, et. al, [PoS Latice2019]

Review of lattice calculations of radiative leptonic decays

Lattice 2019
present first results

CFK, et. al, [arXiv:1907.00279]

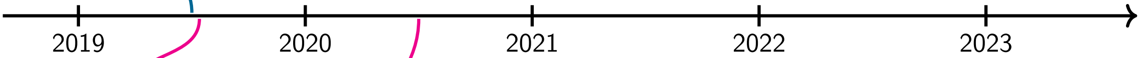

Lattice 2019
present first results

G. Martinelli, et. al, [PoS Latice2019]

physical calculation
for π, K, D, D_s
limited photon energy
range for $D_{(s)}$

Desiderio, et. al, [PRD 2021, arXiv:2006.05358]

Review of lattice calculations of radiative leptonic decays

Lattice 2019
present first results

CFK, et. al, [arXiv:1907.00279]

2019 2020 2021 2022 2023

Lattice 2019
present first results

G. Martinelli, et. al, [PoS Latice2019]

physical calculation
for π, K, D, D_s
limited photon energy
range for $D_{(s)}$

Desiderio, et. al, [PRD 2021, arXiv:2006.05358]

Comparison to
experiment for π, K

Frezzotti, et. al, [PRD 2021, arXiv:2012.02120]

Review of lattice calculations of radiative leptonic decays

Lattice 2019
present first results

CFK, et. al, [arXiv:1907.00279]

2019 2020 2021 2022 2023

Lattice 2019
present first results

G. Martinelli, et. al, [PoS Latice2019]

physical calculation
for π, K, D, D_s
limited photon energy
range for $D_{(s)}$

Desiderio, et. al, [PRD 2021, arXiv:2006.05358]

Comparison to
experiment for π, K

Frezzotti, et. al, [PRD 2021, arXiv:2012.02120]

tension with
$K \to \mu\nu_\mu\gamma$, $\pi \to e\nu_e\gamma$

Review of lattice calculations of radiative leptonic decays

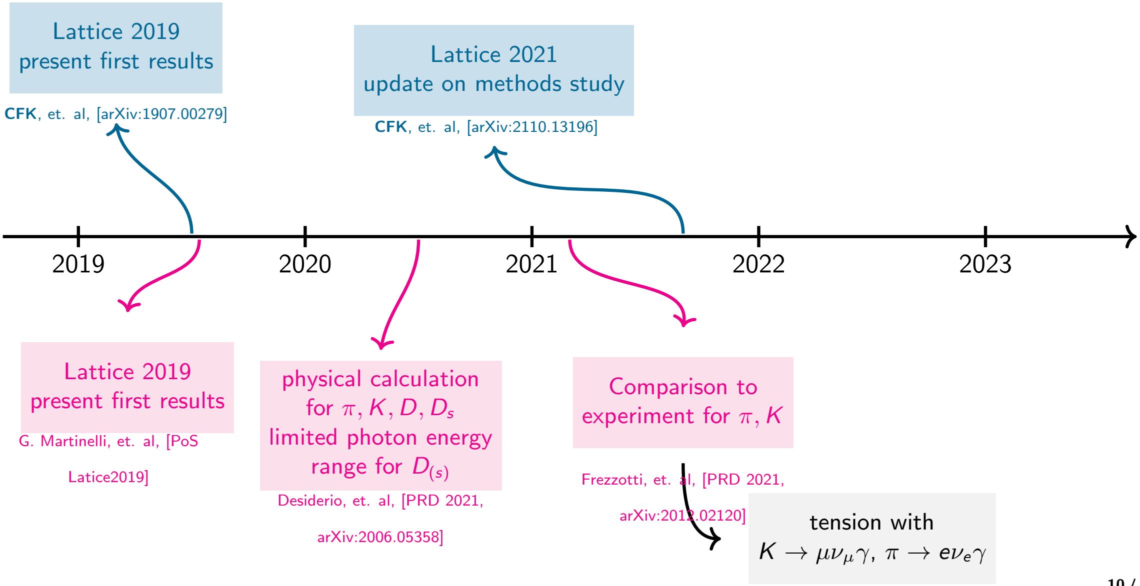

Review of lattice calculations of radiative leptonic decays

Lattice 2019
present first results

CFK, et. al, [arXiv:1907.00279]

Lattice 2021
update on methods study

CFK, et. al, [arXiv:2110.13196]

Methods
paper

D. Giusti, **CFK**, et. al, PRD 2023, arXiv:2302.01298]

2019 2020 2021 2022 2023

Lattice 2019
present first results

G. Martinelli, et. al, [PoS Latice2019]

physical calculation
for π, K, D, D_s
limited photon energy
range for $D_{(s)}$

Desiderio, et. al, [PRD 2021, arXiv:2006.05358]

Comparison to
experiment for π, K

Frezzotti, et. al, [PRD 2021, arXiv:2012.02120]

tension with
$K \to \mu\nu_\mu\gamma$, $\pi \to e\nu_e\gamma$

Review of lattice calculations of radiative leptonic decays

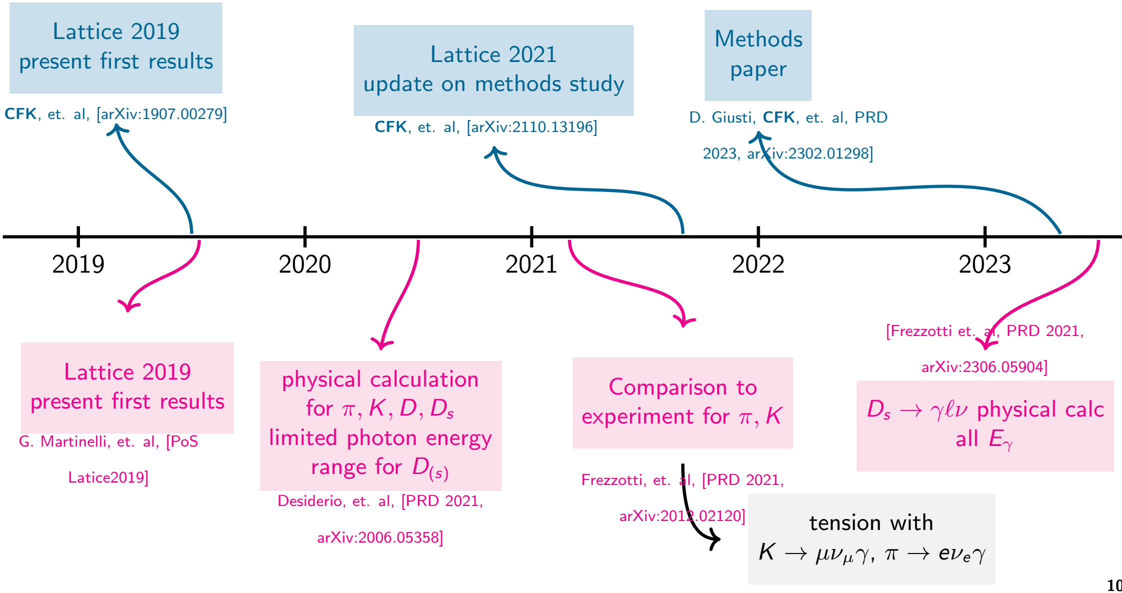

Review of lattice calculations of radiative leptonic decays

Lattice 2019
present first results

CFK, et. al, [arXiv:1907.00279]

Lattice 2021
update on methods study

CFK, et. al, [arXiv:2110.13196]

Methods
paper

D. Giusti, **CFK**, et. al, PRD 2023, arXiv:2302.01298]

Prelim $D_s \to \ell \nu_\ell \gamma$
results

Today

2019

2020

2021

2022

2023

Lattice 2019
present first results

G. Martinelli, et. al, [PoS Latice2019]

physical calculation
for π, K, D, D_s
limited photon energy
range for $D_{(s)}$

Desiderio, et. al, [PRD 2021, arXiv:2006.05358]

Comparison to
experiment for π, K

Frezzotti, et. al, [PRD 2021, arXiv:2012.02120]

tension with
$K \to \mu \nu_\mu \gamma$, $\pi \to e \nu_e \gamma$

[Frezzotti et. al, PRD 2021, arXiv:2306.05904]

$D_s \to \gamma \ell \nu$ physical calc
all E_γ

Outline for section 2

Decay amplitude

To calculate decay amplitude:

- use effective Hamiltonian for weak current
- use 1st order perturbation theory for QED piece

Decay amplitude

To calculate decay amplitude:

- use effective Hamiltonian for weak current
- use 1st order perturbation theory for QED piece

Decay amplitude given by

$$\mathcal{A} = \frac{G_F V_{cs}}{\sqrt{2}} \left[e\epsilon_\mu^* \bar{\ell}\gamma_\nu(1-\gamma_5)\nu \cdot T^{\mu\nu} - ieQ_\ell f_{D_s} \cdot \bar{\ell}\epsilon_\mu^*\gamma^\mu(1-\gamma_5)\nu \right]$$

QCD physics left to calculate is Hadronic tensor $T_{\mu\nu}$

Hadronic Tensor and Form Factors

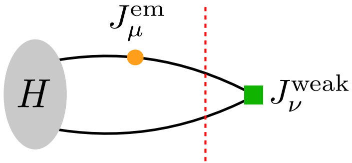

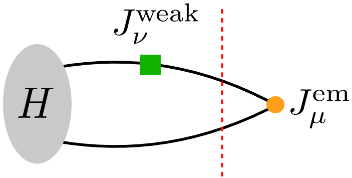

$$J_\mu^{em} = \sum_q e_q \bar{q} \gamma_\mu q, \qquad J_\nu^{weak} = \bar{q}_1 \gamma_\nu (1 - \gamma_5) q_2$$

$$T_{\mu\nu} = -i \int d^4x \; e^{ip_\gamma \cdot x} \langle 0 | \mathbf{T} \left(J_\mu^{\mathrm{em}}(x) J_\nu^{\mathrm{weak}}(0) \right) | H(\vec{p}_H) \rangle$$

Hadronic Tensor and Form Factors

$$J_\mu^{em} = \sum_q e_q \bar{q}\gamma_\mu q, \qquad J_\nu^{weak} = \bar{q}_1\gamma_\nu(1-\gamma_5)q_2$$

$$\begin{aligned} T_{\mu\nu} &= -i\int d^4x\ e^{ip_\gamma\cdot x}\langle 0|\mathbf{T}\left(J_\mu^{\text{em}}(x)J_\nu^{\text{weak}}(0)\right)|H(\vec{p}_H)\rangle \\ &= \epsilon_{\mu\nu\tau\rho}p_\gamma^\tau v^\rho F_V + i\left[-g_{\mu\nu}(v\cdot p_\gamma)+v_\mu(p_\gamma)_\nu\right]F_A - i\frac{v_\mu v_\nu}{(v\cdot p_\gamma)}m_H f_H + (p_\gamma)_\mu\text{-terms} \end{aligned}$$

Hadronic Tensor and Form Factors

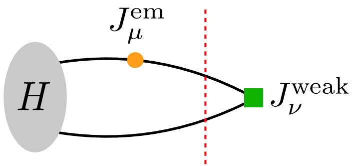

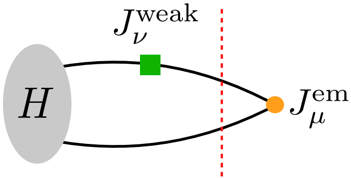

$$J_\mu^{em} = \sum_q e_q \bar{q}\gamma_\mu q, \qquad J_\nu^{weak} = \bar{q}_1\gamma_\nu(1-\gamma_5)q_2$$

$$T_{\mu\nu} = -i\int d^4x\ e^{ip_\gamma\cdot x}\langle 0|\mathbf{T}\left(J_\mu^{\rm em}(x)J_\nu^{\rm weak}(0)\right)|H(\vec{p}_H)\rangle$$

$$= \epsilon_{\mu\nu\tau\rho}p_\gamma^\tau v^\rho F_V + i\big[-g_{\mu\nu}(v\cdot p_\gamma) + v_\mu(p_\gamma)_\nu\big]F_A - i\frac{v_\mu v_\nu}{(v\cdot p_\gamma)}m_H f_H + (p_\gamma)_\mu\text{-terms}$$

$$F_{A,SD} = F_A - (-Q_\ell f_H/E_\gamma^{(0)}), \qquad E_\gamma^{(0)} = p_B\cdot p_\gamma/m_B$$

Hadronic Tensor and Form Factors

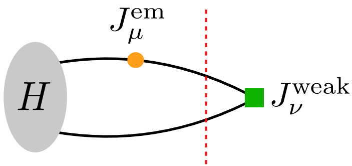

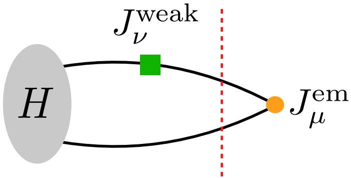

$$J_\mu^{em} = \sum_q e_q \bar{q}\gamma_\mu q, \qquad J_\nu^{weak} = \bar{q}_1\gamma_\nu(1-\gamma_5)q_2$$

$$T_{\mu\nu} = -i\int d^4x\ e^{ip_\gamma\cdot x}\langle 0|\mathbf{T}\left(J_\mu^{\rm em}(x)J_\nu^{\rm weak}(0)\right)|H(\vec{p}_H)\rangle$$

$$= \epsilon_{\mu\nu\tau\rho}p_\gamma^\tau v^\rho F_V + i\big[-g_{\mu\nu}(v\cdot p_\gamma) + v_\mu(p_\gamma)_\nu\big]F_A - i\frac{v_\mu v_\nu}{(v\cdot p_\gamma)}m_H f_H + (p_\gamma)_\mu\text{-terms}$$

$$F_{A,SD} = F_A - (-Q_\ell f_H/E_\gamma^{(0)}), \qquad E_\gamma^{(0)} = p_B\cdot p_\gamma/m_B$$

Goal: Calculate F_V and $F_{A,SD}$ as a function of $E_\gamma^{(0)}$

Euclidean correlation function

(* all times are now Euclidean)

$$C_{3,\mu\nu}(t_{em}, t_H) = \int d^3x \int d^3y \; e^{-i\vec{p}_\gamma\cdot\vec{x}} e^{i\vec{p}_H\cdot\vec{y}} \langle J_\mu^{\text{em}}(t_{em}, \vec{x}) J_\nu^{\text{weak}}(0) \phi_H^\dagger(t_H, \vec{y}) \rangle$$

$$\phi_H^\dagger \sim \bar{Q}\gamma_5 u$$

Euclidean correlation function

(* all times are now Euclidean)

$$C_{3,\mu\nu}(t_{em}, t_H) = \int d^3x \int d^3y \; e^{-i\vec{p}_\gamma\cdot\vec{x}} e^{i\vec{p}_H\cdot\vec{y}} \langle J_\mu^{\rm em}(t_{em}, \vec{x}) J_\nu^{\rm weak}(0) \phi_H^\dagger(t_H, \vec{y}) \rangle$$

$$\phi_H^\dagger \sim \bar{Q}\gamma_5 u$$

Define time-integrated correlation functions for each time ordering

Euclidean correlation function

(* all times are now Euclidean)

$$C_{3,\mu\nu}(t_{em}, t_H) = \int d^3x \int d^3y \; e^{-i\vec{p}_\gamma\cdot\vec{x}} e^{i\vec{p}_H\cdot\vec{y}} \langle J_\mu^{\text{em}}(t_{em}, \vec{x}) J_\nu^{\text{weak}}(0) \phi_H^\dagger(t_H, \vec{y}) \rangle$$

$$\phi_H^\dagger \sim \bar{Q}\gamma_5 u$$

Define time-integrated correlation functions for each time ordering

$$I_{\mu\nu}^{<}(T, t_H) = \int_{-T}^{0} dt_{em} e^{E_\gamma t_{em}} C_{3,\mu\nu}(t_{em}, t_H)$$

$$I_{\mu\nu}^{>}(T, t_H) = \int_{0}^{T} dt_{em} e^{E_\gamma t_{em}} C_{3,\mu\nu}(t_{em}, t_H)$$

Euclidean correlation function

(* all times are now Euclidean)

$$C_{3,\mu\nu}(t_{em}, t_H) = \int d^3x \int d^3y \; e^{-i\vec{p}_\gamma \cdot \vec{x}} e^{i\vec{p}_H \cdot \vec{y}} \langle J_\mu^{\text{em}}(t_{em}, \vec{x}) J_\nu^{\text{weak}}(0) \phi_H^\dagger(t_H, \vec{y}) \rangle$$

$$\phi_H^\dagger \sim \bar{Q}\gamma_5 u$$

Define time-integrated correlation functions for each time ordering

$$I_{\mu\nu}^{<}(T, t_H) = \int_{-T}^{0} dt_{em} e^{E_\gamma t_{em}} C_{3,\mu\nu}(t_{em}, t_H)$$

$$I_{\mu\nu}^{>}(T, t_H) = \int_{0}^{T} dt_{em} e^{E_\gamma t_{em}} C_{3,\mu\nu}(t_{em}, t_H)$$

Show relation between $I_{\mu\nu}(T, t_H)$ and $T_{\mu\nu}$

$\rightarrow$ compare spectral decompositions of both time orderings of $I_{\mu\nu}$ and $T_{\mu\nu}$

Euclidean spectral decomposition of $I^{>}_{\mu\nu}$

Time ordering: $t_{em} > 0$

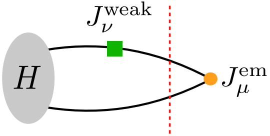

$$T^{>}_{\mu\nu} = \sum_n \frac{\langle 0|J_\mu^{em}(0)|n(\vec{p}_\gamma)\rangle\langle n(\vec{p}_\gamma)|J_\nu^{weak}(0)|H(\vec{p}_H)\rangle}{2E_{n,\vec{p}_\gamma}(E_\gamma - E_{n,\vec{p}_\gamma})}$$

Euclidean spectral decomposition of $I^{>}_{\mu\nu}$

Time ordering: $t_{em} > 0$

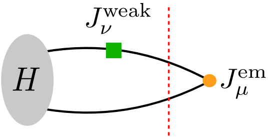

$$T^{>}_{\mu\nu} = \sum_n \frac{\langle 0|J^{em}_{\mu}(0)|n(\vec{p}_\gamma)\rangle\langle n(\vec{p}_\gamma)|J^{weak}_{\nu}(0)|H(\vec{p}_H)\rangle}{2E_{n,\vec{p}_\gamma}(E_\gamma - E_{n,\vec{p}_\gamma})}$$

$$I^{>}_{\mu\nu}(t_H, T) = \int_0^T dt_{em}\ e^{E_\gamma t_{em}} C_{\mu\nu}(t_{em}, t_H)$$

Euclidean spectral decomposition of $I^{>}_{\mu\nu}$

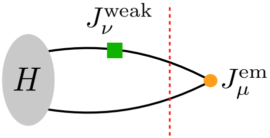

Time ordering: $t_{em} > 0$

$$T^{>}_{\mu\nu} = \sum_n \frac{\langle 0|J^{em}_\mu(0)|n(\vec{p}_\gamma)\rangle\langle n(\vec{p}_\gamma)|J^{weak}_\nu(0)|H(\vec{p}_H)\rangle}{2E_{n,\vec{p}_\gamma}(E_\gamma - E_{n,\vec{p}_\gamma})}$$

$$I^{>}_{\mu\nu}(t_H, T) = \int_0^T dt_{em}\ e^{E_\gamma t_{em}} C_{\mu\nu}(t_{em}, t_H)$$

$$= \sum_m e^{E_m t_H} \frac{\langle m(\vec{p}_H)|\phi^\dagger_H(0)|0\rangle}{2E_{m,\vec{p}_H}}$$

$$\times \sum_n \frac{\langle 0|J^{em}_\mu(0)|n(\vec{p}_\gamma)\rangle\langle n(\vec{p}_\gamma)|J^{weak}_\nu(0)|m(\vec{p}_H)\rangle}{2E_{n,\vec{p}_\gamma}(E_\gamma - E_{n,\vec{p}_\gamma})}\left[1 - e^{(E_\gamma - E_{n,\vec{p}_\gamma})T}\right]$$

Euclidean spectral decomposition of $I^{>}_{\mu\nu}$

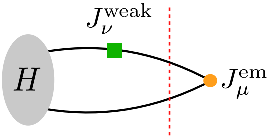

Time ordering: $t_{em} > 0$

$$T^{>}_{\mu\nu} = \sum_n \frac{\langle 0|J^{em}_\mu(0)|n(\vec{p}_\gamma)\rangle\langle n(\vec{p}_\gamma)|J^{weak}_\nu(0)|H(\vec{p}_H)\rangle}{2E_{n,\vec{p}_\gamma}(E_\gamma - E_{n,\vec{p}_\gamma})}$$

$$I^{>}_{\mu\nu}(t_H, T) = \int_0^T dt_{em}\; e^{E_\gamma t_{em}} C_{\mu\nu}(t_{em}, t_H)$$

$t_H \to -\infty$ to achieve ground state saturation

$$= \sum_m e^{E_m t_H} \frac{\langle m(\vec{p}_H)|\phi^\dagger_H(0)|0\rangle}{2E_{m,\vec{p}_H}}$$

$$\times \sum_n \frac{\langle 0|J^{em}_\mu(0)|n(\vec{p}_\gamma)\rangle\langle n(\vec{p}_\gamma)|J^{weak}_\nu(0)|m(\vec{p}_H)\rangle}{2E_{n,\vec{p}_\gamma}(E_\gamma - E_{n,\vec{p}_\gamma})}\left[1 - e^{(E_\gamma - E_{n,\vec{p}_\gamma})T}\right]$$

Euclidean spectral decomposition of $I^{>}_{\mu\nu}$

Time ordering: $t_{em} > 0$

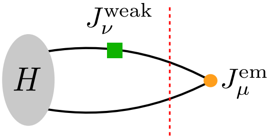

$$T^{>}_{\mu\nu} = \sum_n \frac{\langle 0|J^{em}_\mu(0)|n(\vec{p}_\gamma)\rangle\langle n(\vec{p}_\gamma)|J^{weak}_\nu(0)|H(\vec{p}_H)\rangle}{2E_{n,\vec{p}_\gamma}(E_\gamma - E_{n,\vec{p}_\gamma})}$$

$$I^{>}_{\mu\nu}(t_H, T) = \int_0^T dt_{em}\ e^{E_\gamma t_{em}} C_{\mu\nu}(t_{em}, t_H)$$

$t_H \to -\infty$ to achieve ground state saturation

$$= \sum_m e^{E_m t_H} \frac{\langle m(\vec{p}_H)|\phi^\dagger_H(0)|0\rangle}{2E_{m,\vec{p}_H}}$$

$$\times \sum_n \frac{\langle 0|J^{em}_\mu(0)|n(\vec{p}_\gamma)\rangle\langle n(\vec{p}_\gamma)|J^{weak}_\nu(0)|m(\vec{p}_H)\rangle}{2E_{n,\vec{p}_\gamma}(E_\gamma - E_{n,\vec{p}_\gamma})}\left[1 - e^{(E_\gamma - E_{n,\vec{p}_\gamma})T}\right]$$

- Require $E_\gamma - E_{n,\vec{p}_\gamma} < 0$
- Because the states $|n(\vec{p}_\gamma)\rangle$ have mass, $\sqrt{m_n^2 + \vec{p}_\gamma^2} > |\vec{p}_\gamma|$ is automatically satisfied

Euclidean spectral decomposition of $I^{>}_{\mu\nu}$

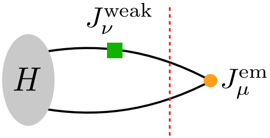

Time ordering: $t_{em} > 0$

$$T^{>}_{\mu\nu} = \sum_n \frac{\langle 0|J^{em}_\mu(0)|n(\vec{p}_\gamma)\rangle\langle n(\vec{p}_\gamma)|J^{weak}_\nu(0)|H(\vec{p}_H)\rangle}{2E_{n,\vec{p}_\gamma}(E_\gamma - E_{n,\vec{p}_\gamma})}$$

$$I^{>}_{\mu\nu}(t_H, T) = \int_0^T dt_{em}\; e^{E_\gamma t_{em}} C_{\mu\nu}(t_{em}, t_H)$$

$t_H \to -\infty$ to achieve ground state saturation

$$= \sum_m e^{E_m t_H} \frac{\langle m(\vec{p}_H)|\phi^\dagger_H(0)|0\rangle}{2E_{m,\vec{p}_H}}$$

$T \to \infty$ to remove unwanted exponentials that come with intermediate states

$$\times \sum_n \frac{\langle 0|J^{em}_\mu(0)|n(\vec{p}_\gamma)\rangle\langle n(\vec{p}_\gamma)|J^{weak}_\nu(0)|m(\vec{p}_H)\rangle}{2E_{n,\vec{p}_\gamma}(E_\gamma - E_{n,\vec{p}_\gamma})}\left[1 - e^{(E_\gamma - E_{n,\vec{p}_\gamma})T}\right]$$

- Require $E_\gamma - E_{n,\vec{p}_\gamma} < 0$
- Because the states $|n(\vec{p}_\gamma)\rangle$ have mass, $\sqrt{m_n^2 + \vec{p}_\gamma^2} > |\vec{p}_\gamma|$ is automatically satisfied

Final relation

For $\mathbf{p}_\gamma \neq \mathbf{0}$,

$$T_{\mu\nu} = \lim_{T\to\infty} \lim_{t_H\to-\infty} \frac{-2E_H e^{-E_H t_H}}{\langle H(\vec{p}_H)|\phi_H^\dagger|0\rangle} \underbrace{\int_{-T}^{T} dt_{em}\ e^{E_\gamma t_{em}} C_{3,\mu\nu}(t_{em}, t_H)}_{I_{\mu\nu}(T, t_H)}$$

Outline for section 3

Calculating $I_{\mu\nu}(T, t_H)$

$$T_{\mu\nu} = \lim_{T\to\infty} \lim_{t_H\to-\infty} \frac{-2E_H e^{-E_H t_H}}{\langle H(\vec{p}_H)|\phi_H^\dagger|0\rangle} \underbrace{\int_{-T}^{T} dt_{em}\ e^{E_\gamma t_{em}} C_{3,\mu\nu}(t_{em}, t_H)}_{I_{\mu\nu}(T,t_H)}$$

Two methods to calculate $I_{\mu\nu}(T, t_H)$:

Calculating $I_{\mu\nu}(T, t_H)$

$$T_{\mu\nu} = \lim_{T\to\infty} \lim_{t_H\to-\infty} \frac{-2E_H e^{-E_H t_H}}{\langle H(\vec{p}_H)|\phi_H^\dagger|0\rangle} \underbrace{\int_{-T}^{T} dt_{em} \; e^{E_\gamma t_{em}} C_{3,\mu\nu}(t_{em}, t_H)}_{I_{\mu\nu}(T,t_H)}$$

Two methods to calculate $I_{\mu\nu}(T, t_H)$:

1: 3d (timeslice) sequential propagator through $\phi_H^\dagger$ $\rightarrow$ calculate $C_{3,\mu\nu}(t_{em}, t_H)$ on lattice, fixed t_H get all t_{em} for free

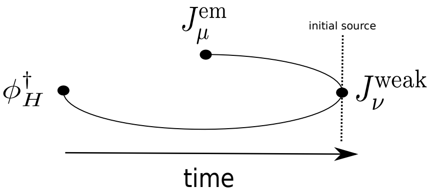

Calculating $I_{\mu\nu}(T, t_H)$

$$T_{\mu\nu} = \lim_{T\to\infty} \lim_{t_H\to-\infty} \frac{-2E_H e^{-E_H t_H}}{\langle H(\vec{p}_H)|\phi_H^\dagger|0\rangle} \underbrace{\int_{-T}^{T} dt_{em}\ e^{E_\gamma t_{em}} C_{3,\mu\nu}(t_{em}, t_H)}_{I_{\mu\nu}(T,t_H)}$$

Two methods to calculate $I_{\mu\nu}(T, t_H)$:

1: 3d (timeslice) sequential propagator through $\phi_H^\dagger \to$ calculate $C_{3,\mu\nu}(t_{em}, t_H)$ on lattice, fixed t_H get all t_{em} for free

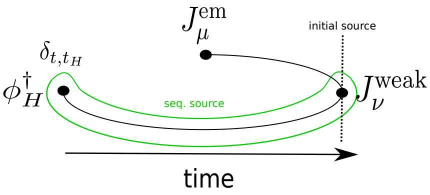

Calculating $I_{\mu\nu}(T, t_H)$

$$T_{\mu\nu} = \lim_{T\to\infty} \lim_{t_H\to-\infty} \frac{-2E_H e^{-E_H t_H}}{\langle H(\vec{p}_H)|\phi_H^\dagger|0\rangle} \underbrace{\int_{-T}^{T} dt_{em}\ e^{E_\gamma t_{em}} C_{3,\mu\nu}(t_{em}, t_H)}_{I_{\mu\nu}(T,t_H)}$$

Two methods to calculate $I_{\mu\nu}(T, t_H)$:

1: 3d (timeslice) sequential propagator through $\phi_H^\dagger \to$ calculate $C_{3,\mu\nu}(t_{em}, t_H)$ on lattice, fixed t_H get all t_{em} for free

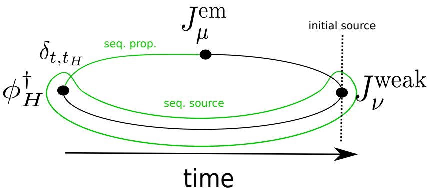

Calculating $I_{\mu\nu}(T, t_H)$

$$T_{\mu\nu} = \lim_{T\to\infty} \lim_{t_H\to-\infty} \frac{-2E_H e^{-E_H t_H}}{\langle H(\vec{p}_H)|\phi_H^\dagger|0\rangle} \underbrace{\int_{-T}^{T} dt_{em}\; e^{E_\gamma t_{em}} C_{3,\mu\nu}(t_{em}, t_H)}_{I_{\mu\nu}(T,t_H)}$$

Two methods to calculate $I_{\mu\nu}(T, t_H)$:

1: 3d (timeslice) sequential propagator through $\phi_H^\dagger \rightarrow$ calculate $C_{3,\mu\nu}(t_{em}, t_H)$ on lattice, fixed t_H get all t_{em} for free

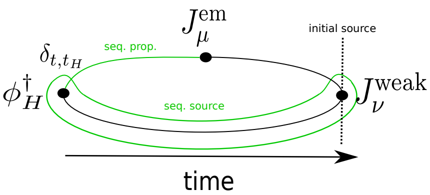

2: 4d sequential propagator through $J_\mu^{em} \rightarrow$ calculate $I_{\mu\nu}(T, t_H)$ on lattice, fixed T get all t_H for free

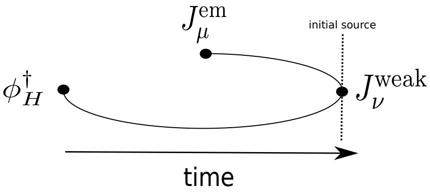

Calculating $I_{\mu\nu}(T, t_H)$

$$T_{\mu\nu} = \lim_{T\to\infty} \lim_{t_H\to-\infty} \frac{-2E_H e^{-E_H t_H}}{\langle H(\vec{p}_H)|\phi_H^\dagger|0\rangle} \underbrace{\int_{-T}^{T} dt_{em}\ e^{E_\gamma t_{em}} C_{3,\mu\nu}(t_{em}, t_H)}_{I_{\mu\nu}(T,t_H)}$$

Two methods to calculate $I_{\mu\nu}(T, t_H)$:

1: 3d (timeslice) sequential propagator through $\phi_H^\dagger \to$ calculate $C_{3,\mu\nu}(t_{em}, t_H)$ on lattice, fixed t_H get all t_{em} for free

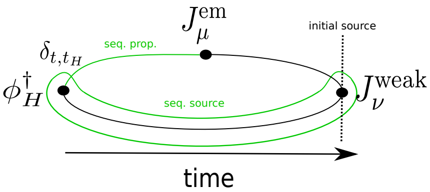

2: 4d sequential propagator through $J_\mu^{em} \to$ calculate $I_{\mu\nu}(T, t_H)$ on lattice, fixed T get all t_H for free

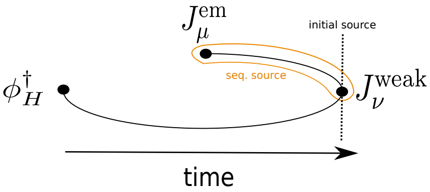

Calculating $I_{\mu\nu}(T, t_H)$

$$T_{\mu\nu} = \lim_{T\to\infty} \lim_{t_H\to-\infty} \frac{-2E_H e^{-E_H t_H}}{\langle H(\vec{p}_H)|\phi_H^\dagger|0\rangle} \underbrace{\int_{-T}^{T} dt_{em}\ e^{E_\gamma t_{em}} C_{3,\mu\nu}(t_{em}, t_H)}_{I_{\mu\nu}(T,t_H)}$$

Two methods to calculate $I_{\mu\nu}(T, t_H)$:

1: 3d (timeslice) sequential propagator through $\phi_H^\dagger \to$ calculate $C_{3,\mu\nu}(t_{em}, t_H)$ on lattice, fixed t_H get all t_{em} for free

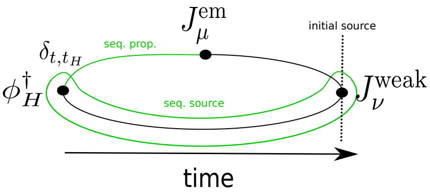

2: 4d sequential propagator through $J_\mu^{em} \to$ calculate $I_{\mu\nu}(T, t_H)$ on lattice, fixed T get all t_H for free

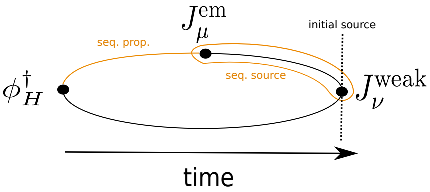

Calculating $I_{\mu\nu}(T, t_H)$

$$T_{\mu\nu} = \lim_{T\to\infty} \lim_{t_H\to-\infty} \frac{-2E_H e^{-E_H t_H}}{\langle H(\vec{p}_H)|\phi_H^\dagger|0\rangle} \underbrace{\int_{-T}^{T} dt_{em}\; e^{E_\gamma t_{em}} C_{3,\mu\nu}(t_{em}, t_H)}_{I_{\mu\nu}(T,t_H)}$$

Two methods to calculate $I_{\mu\nu}(T, t_H)$:

1: 3d (timeslice) sequential propagator through $\phi_H^\dagger$ $\rightarrow$ calculate $C_{3,\mu\nu}(t_{em}, t_H)$ on lattice, fixed t_H get all t_{em} for free

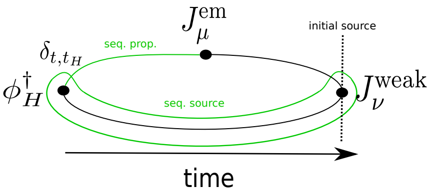

2: 4d sequential propagator through J_μ^{em} $\rightarrow$ calculate $I_{\mu\nu}(T, t_H)$ on lattice, fixed T get all t_H for free

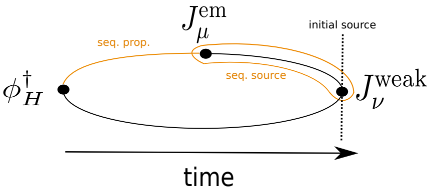

Limitation of 4d method: cannot resolve time orderings

Calculating $I_{\mu\nu}(T, t_H)$

$$T_{\mu\nu} = \lim_{T\to\infty} \lim_{t_H\to-\infty} \frac{-2E_H e^{-E_H t_H}}{\langle H(\vec{p}_H)|\phi_H^\dagger|0\rangle} \underbrace{\int_{-T}^{T} dt_{em}\ e^{E_\gamma t_{em}} C_{3,\mu\nu}(t_{em}, t_H)}_{I_{\mu\nu}(T,t_H)}$$

Two methods to calculate $I_{\mu\nu}(T, t_H)$:

1: 3d (timeslice) sequential propagator through $\phi_H^\dagger \to$ calculate $C_{3,\mu\nu}(t_{em}, t_H)$ on lattice, fixed t_H get all t_{em} for free

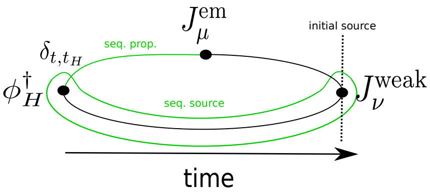

2: 4d sequential propagator through $J_\mu^{em} \to$ calculate $I_{\mu\nu}(T, t_H)$ on lattice, fixed T get all t_H for free

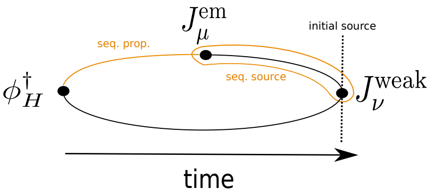

Limitation of 4d method: cannot resolve time orderings

$\Longrightarrow$ **4d**$^{>,<}$ **method**: perform two sequential solves to resolve $t_{em} < 0$ and $t_{em} > 0$

Past lattice studies

$$T_{\mu\nu} = \lim_{T\to\infty} \lim_{t_H\to-\infty} \frac{-2E_H e^{-E_H t_H}}{\langle H(\vec{p}_H)|\phi_H^\dagger|0\rangle} \underbrace{\int_{-T}^{T} dt_{em}\ e^{E_\gamma t_{em}} C_{3,\mu\nu}(t_{em}, t_H)}_{I_{\mu\nu}(T,t_H)}$$

- [1] we presented results at Lattice 2019 using 3d method
  - fitting to a constant looking for plateaus in T and t_H
- [2, 3] use 4d method to perform realistic physical calculation
  - set $T = N_T/2$ and fit to constant in t_H where data has plateaued
- [4] perform a methods study comparing 3d and 4d methods
  - data does not always plateau in T and t_H
    $\to$ develop fit methods to extrapolate to $T \to \infty$ and $t_H \to -\infty$

[1] [**CFK**, Lehner, Meinel, Soni, arXiv:1907.00279]

[2] [Desiderio, Frezzotti, Garofalo, Giusti, Hansen, Lubicz, Martinelli, Sachrajda, Sanfilippo, Simula, Tantalo, PRD 2021, arXiv:2006.05358]

[3] [Frezzotti, Gagliardi, Lubicz, Martinelli, Mazzetti, Sachrajda, Sanfilippo, Simula, Tantalo, PRD 2021, arXiv:2306.05904]

[4] [D. Giusti, **CFK**, C. Lehner, S. Meinel, A. Soni, PRD 2023 / arXiv:2302.01298]

Comparison of 3d and 4d methods

Show fit methods to take $\lim_{T\to\infty}$ and $\lim_{t_H\to-\infty}$

- fitting only 4d$^{>,<}$ method data
- fitting only 3d method data
- performing global fits to both 3d and 4d$^{>,<}$ method data

Goal: find methods with best control over $\lim_{T\to\infty}$ and $\lim_{t_H\to-\infty}$ limits for cheapest cost

Simulation parameters for 3d/4d method comparison

- $N_f = 2 + 1$ DWF, RBC/UKQCD gauge ensemble

ensemble	$(L/a)^3 \times (T/a)$	L_5/a	$\approx a^{-1}$(GeV)	am_l	am_s	$\approx M_\pi$(MeV)	N_{conf}
24I	$24^3 \times 64$	16	1.785	0.005	0.04	340	25

- Use local currents with mostly non-perturbative renormalization
- charm valence quarks $\rightarrow$ Möbius domain-wall with "stout" smearing
- u/d/s valence quarks $\rightarrow$ same DWF action as sea quarks
- Neglect disconnected diagrams
- Use all-mode averaging with 1 exact and 16 sloppy solves per configuration
- $\mathbb{Z}_2$ random wall sources

Parameters for $D_s \to \gamma\ell\nu$ runs

Meson and photon momenta:

Method	Source	Meson Momentum	Photon Momentum
3d	$\mathbb{Z}_2$-wall	$\vec{p}_{D_s} = (0,0,0)$	$\lvert\vec{p}_\gamma\rvert^2 \in (2\pi/L)^2\{1,2,3,4\}$
4d	$\mathbb{Z}_2$-wall	$\vec{p}_{D_s,z} \in 2\pi/L\{-1,0,1,2\}$	$\vec{p}_{\gamma,z} = 2\pi/L$

4d$^{>,<}$ method:

- 3 values of integration range $T/a \in \{6, 9, 12\}$

3d method:

- 3 values of source-sink separation $t_H/a \in \{-6, -9, -12\}$

Fit form factors $F(t_H, T)$ directly instead of time-integrated correlation function $I_{\mu\nu}(t_H, T)$

Fit form: 4d$^{>,<}$ method

Include terms to fit
(1) unwanted exponential from first intermediate state
(2) first excited state

Fit form: 4d$^{>,<}$ method

Include terms to fit
(1) unwanted exponential from first intermediate state
(2) first excited state

Time ordering $t_{em} > 0$:

$$F^{>}(t_H, T) = F^{>} + B_F^{>}\, e^{(E_\gamma - E^{>})T} + C_F^{>}\, e^{\Delta E t_H}$$

■ fit parameters

Fit form: 4d$^{>,<}$ method

Include terms to fit
(1) unwanted exponential from first intermediate state
(2) first excited state

Time ordering $t_{em} > 0$:

$$F^{>}(t_H, T) = F^{>} + B_F^{>} e^{(E_\gamma - E^{>})T} + C_F^{>} e^{\overbrace{\Delta E t_H}}$$

■ fit parameters

Fit form: 4d$^{>,<}$ method

Include terms to fit
(1) unwanted exponential from first intermediate state
(2) first excited state

Time ordering $t_{em} > 0$:

$$F^{>}(t_H, T) = F^{>} + B_F^{>}\, e^{\overbrace{(E_\gamma - E^{>})T}} + C_F^{>}\, e^{\overbrace{\Delta E t_H}}$$

■ fit parameters

$4d^{>,<}$ method: Fits to F_V for $t_{em} > 0$ time ordering

$$F^{>}(t_H, T) = F^{>} + B_F^{>} \overbrace{e^{(E_\gamma - E^{>})T}} + C_F^{>} \overbrace{e^{\Delta E t_H}}$$

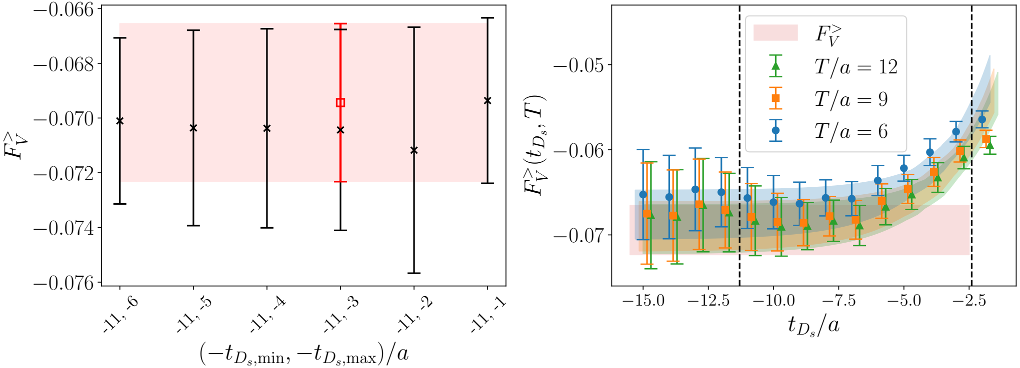

Fit form: 3d method

Include terms to fit
(1) unwanted exponential from first intermediate state
(2) first excited state

Fit form: 3d method

Include terms to fit
(1) unwanted exponential from first intermediate state
(2) first excited state

Time ordering $t_{em} < 0$:

$$F^{<}(t_H, T) = F^{<} + B_F^{<}(1 + B_{F,\mathrm{exc}}^{<}\, e^{\Delta E (T + t_H)})\, e^{-(E_\gamma - E_H + E^{<})T} + C_F^{<}\, e^{\Delta E\, t_H}$$

■ fit parameters

Fit form: 3d method

Include terms to fit
(1) unwanted exponential from first intermediate state
(2) first excited state

Time ordering $t_{em} < 0$:

$$F^{<}(t_H, T) = F^{<} + B_F^{<}(1 + B_{F,\text{exc}}^{<}\, \overbrace{e^{\Delta E (T + t_H)}})\, e^{-(E_\gamma - E_H + E^{<})T} + C_F^{<}\, \overbrace{e^{\Delta E t_H}}$$

■ fit parameters

Fit form: 3d method

Include terms to fit
(1) unwanted exponential from first intermediate state
(2) first excited state

Time ordering $t_{em} < 0$:

$$F^<(t_H, T) = F^< + B_F^<(1 + B_{F,\mathrm{exc}}^< \overbrace{e^{\Delta E(T+t_H)}}) \overbrace{e^{-(E_\gamma - E_H + E^<)T}} + C_F^< \overbrace{e^{\Delta E t_H}}$$

■ fit parameters

Fit form: 3d method

Include terms to fit
(1) unwanted exponential from first intermediate state
(2) first excited state

Time ordering $t_{em} < 0$:

$$F^{<}(t_H, T) = F^{<} + B_F^{<}(1 + B_{F,\text{exc}}^{<}\, \overbrace{e^{\Delta E(T+t_H)}})\, \overbrace{e^{-(E_\gamma - E_H + E^{<})T}} + C_F^{<}\, \overbrace{e^{\Delta E t_H}}$$

■ fit parameters

To help stabilize the fits
→ Determine ΔE from the pseudoscalar two-point correlation function
→ use result as Gaussian prior in form factor fits

3d method: Fits to F_V for $t_{\text{em}} < 0$ time ordering

$$F_V^<(t_{D_s}, T) = F_V^< + B_F^<\big(1 + B_{F,\text{exc}}^< \overbrace{e^{\Delta E(T+t_H)}}\big)\, \overbrace{e^{-(E_\gamma - E_H + E^<)T}} + C_F^< \,\overbrace{e^{\Delta E t_H}}$$

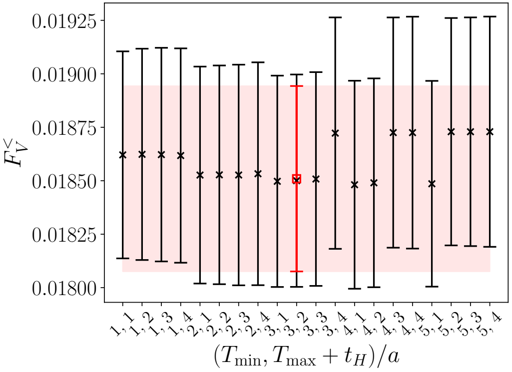

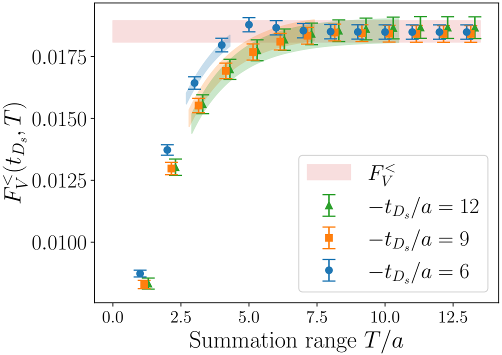

F_V as function of $E_\gamma^{(0)}$ using 3d and 4d methods

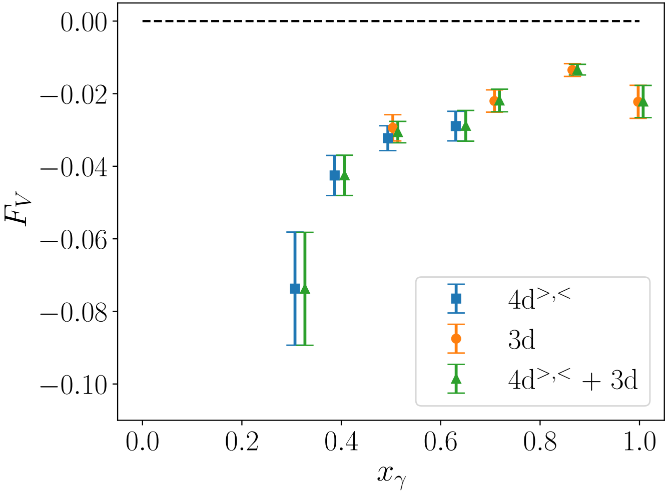

$$x_\gamma = 2E_\gamma^{(0)}/m_{D_s}$$

$$0 \leq x_\gamma \leq 1 - \frac{m_\ell^2}{m_{D_s}^2}$$

F_V as function of $E_\gamma^{(0)}$ using 3d and 4d methods

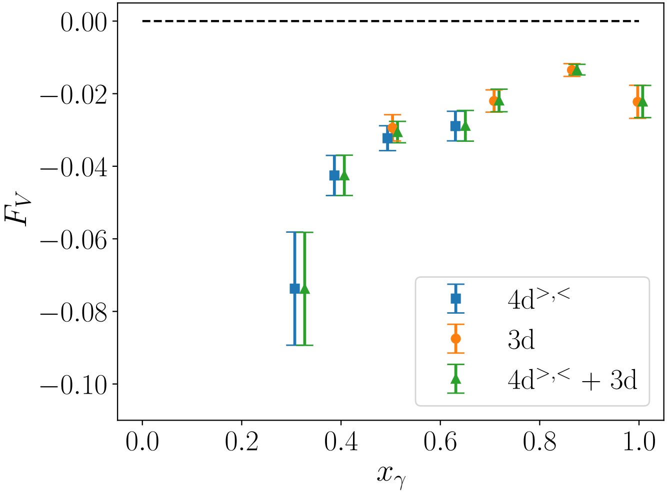

$$x_\gamma = 2E_\gamma^{(0)}/m_{D_s}$$

$$0 \le x_\gamma \le 1 - \frac{m_\ell^2}{m_{D_s}^2}$$

Summary:

F_V as function of $E_\gamma^{(0)}$ using 3d and 4d methods

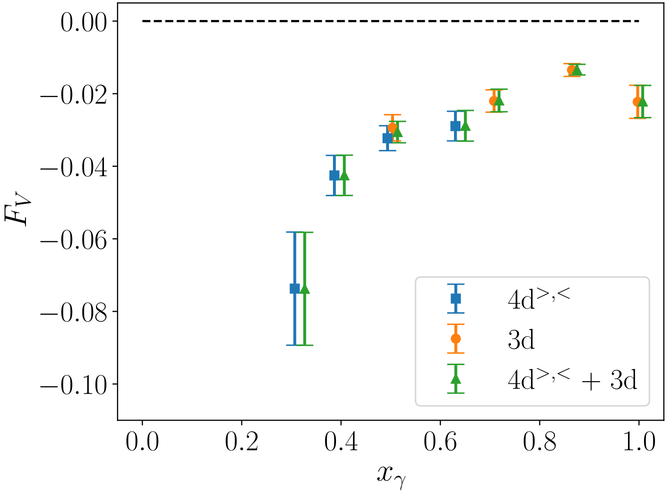

$$x_\gamma = 2E_\gamma^{(0)} / m_{D_s}$$

$$0 \leq x_\gamma \leq 1 - \frac{m_\ell^2}{m_{D_s}^2}$$

Summary:

- 3d and $4\mathrm{d}^{>,<}$ methods offer good control over systematics

F_V as function of $E_\gamma^{(0)}$ using 3d and 4d methods

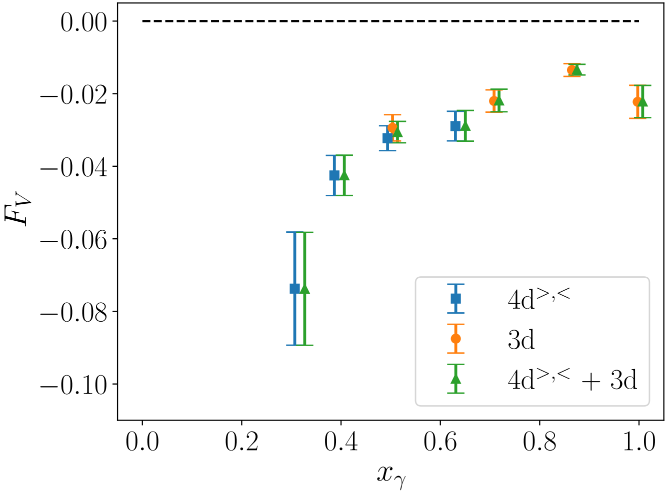

$$x_\gamma = 2E_\gamma^{(0)}/m_{D_s}$$

$$0 \le x_\gamma \le 1 - \frac{m_\ell^2}{m_{D_s}^2}$$

Summary:

- 3d and $4d^{>,<}$ methods offer good control over systematics
- Combined fits offer small improvement relative to individual

F_V as function of $E_\gamma^{(0)}$ using 3d and 4d methods

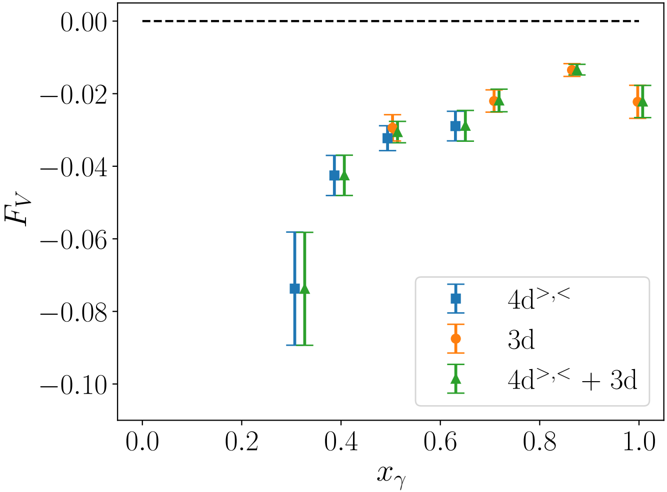

$$x_\gamma = 2E_\gamma^{(0)}/m_{D_s}$$

$$0 \leq x_\gamma \leq 1 - \frac{m_\ell^2}{m_{D_s}^2}$$

Summary:

- 3d and $4d^{>,<}$ methods offer good control over systematics
- Combined fits offer small improvement relative to individual

Compare computational cost of 3d and $4d^{>,<}$ methods

Number of propagator solves per configuration

3d method

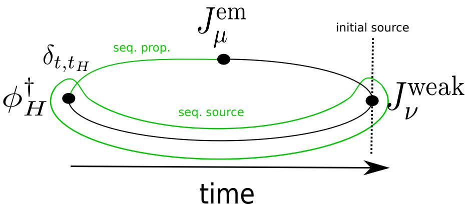

$4d^{>,<}$ method

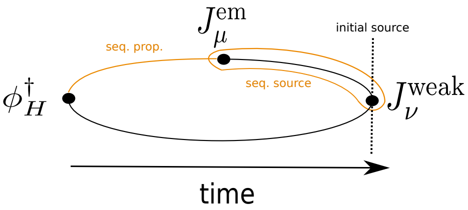

Source	3d	$4d^{>,<}$
point	$2(1 + N_{t_H} N_{p_H})$	
$\mathbb{Z}_2$ wall	$2(1 + N_{t_H} N_{p_H} + N_{p_H} N_{p_\gamma})$	

Number of propagator solves per configuration

3d method

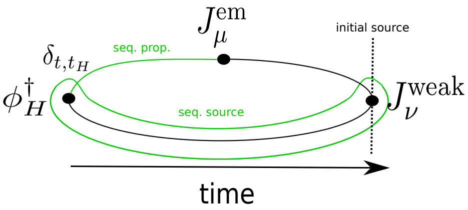

$4d^{>,<}$ method

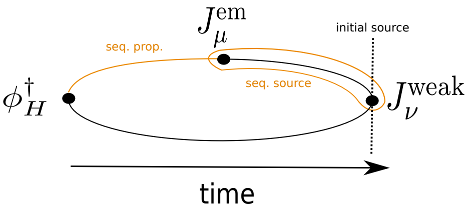

Source	3d	$4d^{>,<}$
point	$2(1 + N_{t_H} N_{p_H})$	$2(1 + 2 \times 4 N_T N_{p_\gamma})$
$\mathbb{Z}_2$ wall	$2(1 + N_{t_H} N_{p_H} + N_{p_H} N_{p_\gamma})$	$2(1 + 2 \times 4 N_T N_{p_\gamma} + N_{p_\gamma} N_{p_H})$

Number of propagator solves per configuration

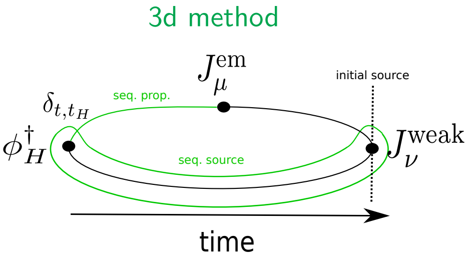

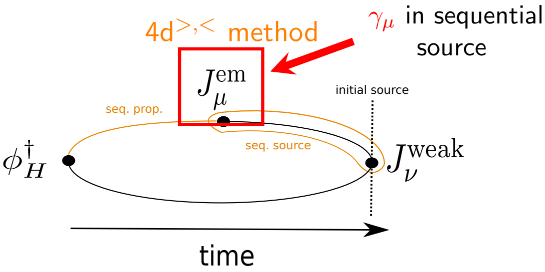

Source	3d	$4d^{>,<}$
point	$2(1 + N_{t_H} N_{p_H})$	$2(1 + 2 \times 4 N_T N_{p_\gamma})$
$\mathbb{Z}_2$ wall	$2(1 + N_{t_H} N_{p_H} + N_{p_H} N_{p_\gamma})$	$2(1 + 2 \times 4 N_T N_{p_\gamma} + N_{p_\gamma} N_{p_H})$

Number of propagator solves per configuration

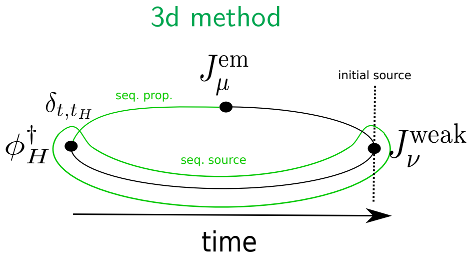

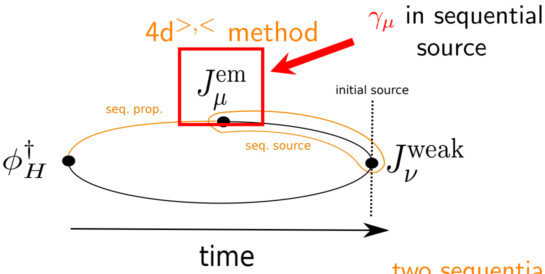

two sequential solves to resolve time orders

Source	3d	$4d^{>,<}$
point	$2(1 + N_{t_H} N_{p_H})$	$2(1 + 2 \times 4 N_T N_{p_\gamma})$
$\mathbb{Z}_2$ wall	$2(1 + N_{t_H} N_{p_H} + N_{p_H} N_{p_\gamma})$	$2(1 + 2 \times 4 N_T N_{p_\gamma} + N_{p_\gamma} N_{p_H})$

Number of propagator solves per configuration

3d method

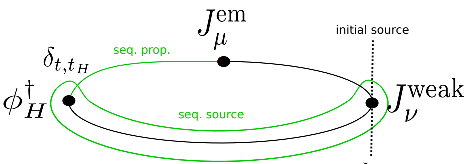

$4d^{>,<}$ method

γ_μ in sequential source

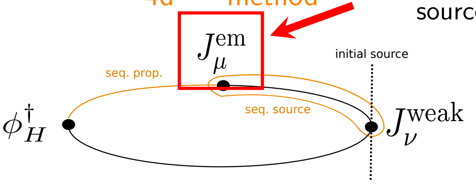

two sequential solves to resolve time orders

Source	3d	$4d^{>,<}$
point	$2(1+N_{t_H}N_{p_H})$	$2(1+2\times 4N_T N_{p_\gamma})$
$\mathbb{Z}_2$ wall	$2(1+N_{t_H}N_{p_H}+N_{p_H}N_{p_\gamma})$	$2(1+2\times 4N_T N_{p_\gamma}+N_{p_\gamma}N_{p_H})$

- $4d^{>,<}$ method generally more expensive than 3d method if cover full $E_\gamma^{(0)}$ range

Number of propagator solves per configuration

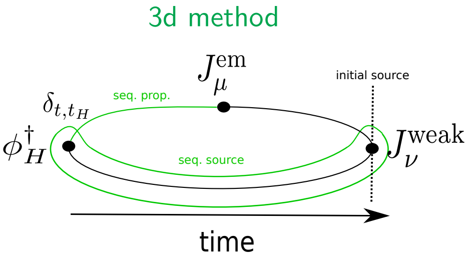

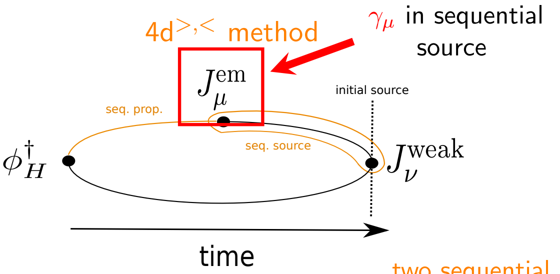

Source	3d	$4\text{d}^{>,<}$
point	$2(1 + N_{t_H} N_{p_H})$	$2(1 + 2 \times 4 N_T N_{p_\gamma})$
$\mathbb{Z}_2$ wall	$2(1 + N_{t_H} N_{p_H} + N_{p_H} N_{p_\gamma})$	$2(1 + 2 \times 4 N_T N_{p_\gamma} + N_{p_\gamma} N_{p_H})$

- $4\text{d}^{>,<}$ method generally more expensive than 3d method if cover full $E_\gamma^{(0)}$ range

3d method offers good control over systematics for cheapest cost

Improved estimators using 3d method

Simulation parameters for final 3d method dataset

- $N_f = 2+1$ DWF, 3 RBC/UKQCD gauge ensembles

ensemble	$(L/a)^3 \times (T/a)$	L_5/a	$\approx a^{-1}$(GeV)	am_l	am_s	$\approx M_\pi$(MeV)	N_{conf}
24I	$24^3 \times 64$	16	1.785	0.005	0.04	340	25
32I	$32^3 \times 64$	16	2.383	0.004	0.03	304	26
48I	$48^3 \times 96$	24	1.730	0.00078	0.0362	139	7

- Use local currents with mostly non-perturbative renormalization
- charm valence quarks → Möbius domain-wall with "stout" smearing
- u/d/s valence quarks → same DWF action as sea quarks
- Neglect disconnected diagrams
- Use all-mode averaging 4 exact and 64 sloppy solves per config

Simulation parameters for final 3d method dataset

- $N_f = 2+1$ DWF, 3 RBC/UKQCD gauge ensembles

ensemble	$(L/a)^3 \times (T/a)$	L_5/a	$\approx a^{-1}$(GeV)	am_l	am_s	$\approx M_\pi$(MeV)	N_{conf}
24I	$24^3 \times 64$	16	1.785	0.005	0.04	340	25
32I	$32^3 \times 64$	16	2.383	0.004	0.03	304	26
48I	$48^3 \times 96$	24	1.730	0.00078	0.0362	139	7

- Use local currents with mostly non-perturbative renormalization
- charm valence quarks $\to$ Möbius domain-wall with "stout" smearing
- u/d/s valence quarks $\to$ same DWF action as sea quarks
- Neglect disconnected diagrams
- Use all-mode averaging 4 exact and 64 sloppy solves per config

Final improved estimators using 3d method:

- $\mathbb{Z}_2$ random wall sources and point sources
- Two datasets: $J_\nu^{\mathrm{weak}}(0)$ or $J_\mu^{\mathrm{em}}(0)$
- For point-sources use translational invariance to fix em/weak operator at origin
  $\to$ use "infinite-volume approximation" to generate data at arbitrary photon momenta (only exponentially small FVEs introduced)

Alternate correlation function

- Fix em current at origin: $J_\mu^{\text{em}}(0)$

$$C^{\text{EM}}_{3,\mu\nu}(t_W, t_H) = \overbrace{e^{E_H t_W}}^{} \int d^3x \int d^3y \; \overbrace{e^{-i\vec{p}_H\cdot\vec{x}}}^{} e^{i\vec{p}_\gamma\cdot\vec{x}} e^{i\vec{p}_H\cdot\vec{y}} \langle J_\mu^{\text{em}}(0) J_\nu^{\text{weak}}(t_W, \vec{x}) \phi_H^\dagger(t_H, \vec{y})\rangle$$

Alternate correlation function

- Fix em current at origin: $J_\mu^{\text{em}}(0)$

$$C_{3,\mu\nu}^{\text{EM}}(t_W, t_H) = \overbrace{e^{E_H t_W}} \int d^3x \int d^3y \; \overbrace{e^{-i\vec{p}_H\cdot\vec{x}}} e^{i\vec{p}_\gamma\cdot\vec{x}} e^{i\vec{p}_H\cdot\vec{y}} \langle J_\mu^{\text{em}}(0) J_\nu^{\text{weak}}(t_W, \vec{x}) \phi_H^\dagger(t_H, \vec{y})\rangle$$

- $e^{E_H t_W}$ and $e^{-i\vec{p}_H\cdot\vec{x}}$ shift weak current relative to other operators

Alternate correlation function

- Fix em current at origin: $J_\mu^{\mathrm{em}}(0)$

$$C_{3,\mu\nu}^{\mathrm{EM}}(t_W, t_H) = \overbrace{e^{E_H t_W}} \int d^3x \int d^3y \; \overbrace{e^{-i\vec{p}_H\cdot\vec{x}}} \, e^{i\vec{p}_\gamma\cdot\vec{x}} e^{i\vec{p}_H\cdot\vec{y}} \langle J_\mu^{\mathrm{em}}(0) J_\nu^{\mathrm{weak}}(t_W, \vec{x}) \phi_H^\dagger(t_H, \vec{y})\rangle$$

- $e^{E_H t_W}$ and $e^{-i\vec{p}_H\cdot\vec{x}}$ shift weak current relative to other operators
- using point sources, can reuse sequential propagators to get for free

Alternate correlation function

- Fix em current at origin: $J_\mu^{\text{em}}(0)$

$$C_{3,\mu\nu}^{\text{EM}}(t_W, t_H) = \overbrace{e^{E_H t_W}} \int d^3x \int d^3y \; \overbrace{e^{-i\vec{p}_H\cdot\vec{x}}} e^{i\vec{p}_\gamma\cdot\vec{x}} e^{i\vec{p}_H\cdot\vec{y}} \langle J_\mu^{\text{em}}(0) J_\nu^{\text{weak}}(t_W, \vec{x}) \phi_H^\dagger(t_H, \vec{y})\rangle$$

- $e^{E_H t_W}$ and $e^{-i\vec{p}_H\cdot\vec{x}}$ shift weak current relative to other operators
- using point sources, can reuse sequential propagators to get for free
- define analogous time-integrated correlation function $I_{\mu\nu}^{<,\text{EM}}(T, t_H)$ and $I_{\mu\nu}^{>,\text{EM}}(T, t_H)$

Alternate correlation function

- Fix em current at origin: $J_\mu^{\text{em}}(0)$

$$C_{3,\mu\nu}^{\text{EM}}(t_W, t_H) = \overbrace{e^{E_H t_W}} \int d^3x \int d^3y \; \overbrace{e^{-i\vec{p}_H\cdot\vec{x}}} \, e^{i\vec{p}_\gamma\cdot\vec{x}} e^{i\vec{p}_H\cdot\vec{y}} \langle J_\mu^{\text{em}}(0) J_\nu^{\text{weak}}(t_W, \vec{x}) \phi_H^\dagger(t_H, \vec{y})\rangle$$

- $e^{E_H t_W}$ and $e^{-i\vec{p}_H\cdot\vec{x}}$ shift weak current relative to other operators
- using point sources, can reuse sequential propagators to get for free
- define analogous time-integrated correlation function $I_{\mu\nu}^{<,\text{EM}}(T, t_H)$ and $I_{\mu\nu}^{>,\text{EM}}(T, t_H)$

Spectral decompositions show us

$$I_{\mu\nu}^{<,\text{EM}}(T, t_H) = I_{\mu\nu}^{>}(T, t_H) + \text{excited state effects}$$

$$I_{\mu\nu}^{>,\text{EM}}(T, t_H) = I_{\mu\nu}^{<}(T, t_H) + \text{excited state effects}$$

Perform combined fits to take advantage of this relation

Alternate correlation function

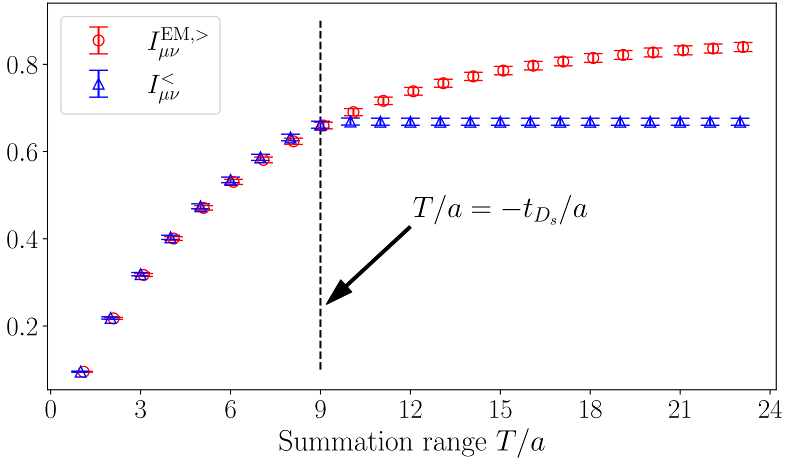

- Can integrate past $T = -t_H$ using alternate correlation function

Alternate correlation function: vector form factor

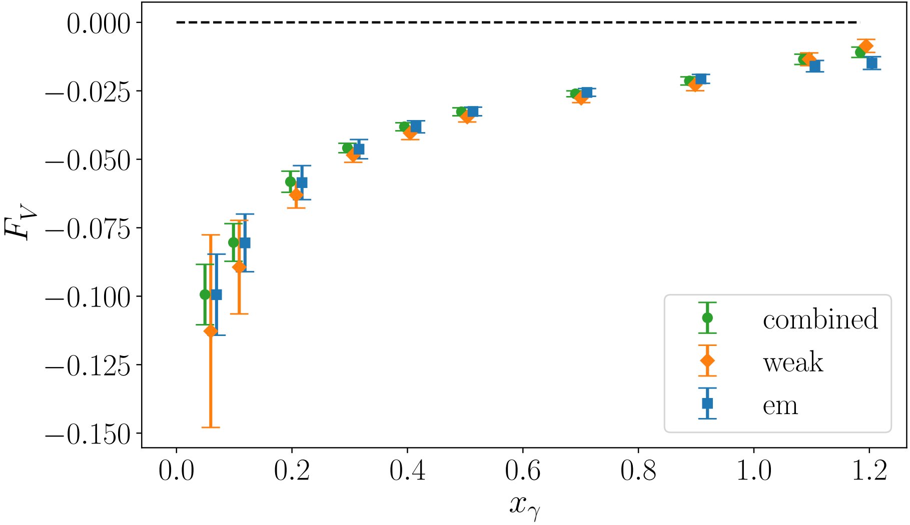

Non-perturbative subtraction of IR divergent lattice artifacts

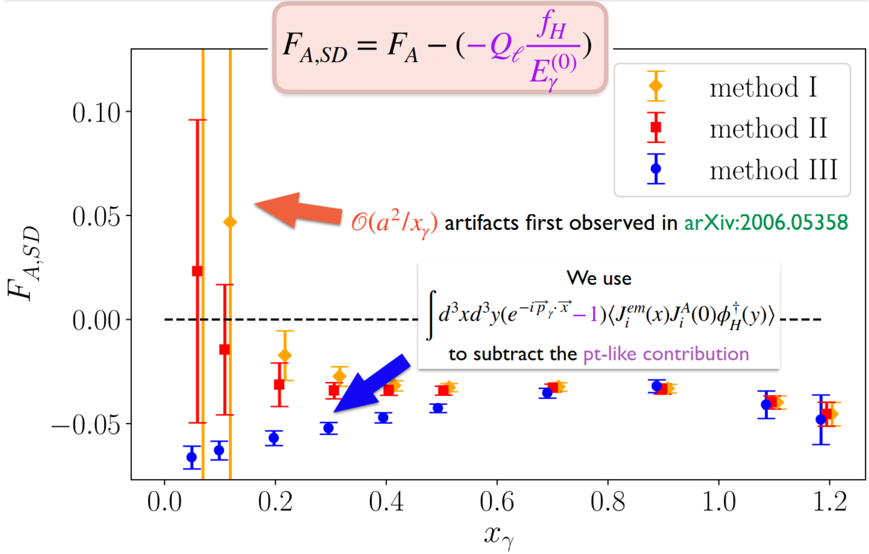

Blue data: improved subtraction of point-like contribution

Taking ratios of correlation functions

$$C_{3,\mu\nu}^{\text{improved}}(\vec{p}_\gamma, t) = C_{3,\mu\nu}^{\text{point}}(\vec{p}_\gamma, t)\frac{C_{3,\mu\nu}^{\mathbb{Z}_2}(\vec{p}^*, t)}{C_{3,\mu\nu}^{\text{point}}(\vec{p}^*, t)}, \qquad \vec{p}^* = \frac{2\pi}{L}n$$

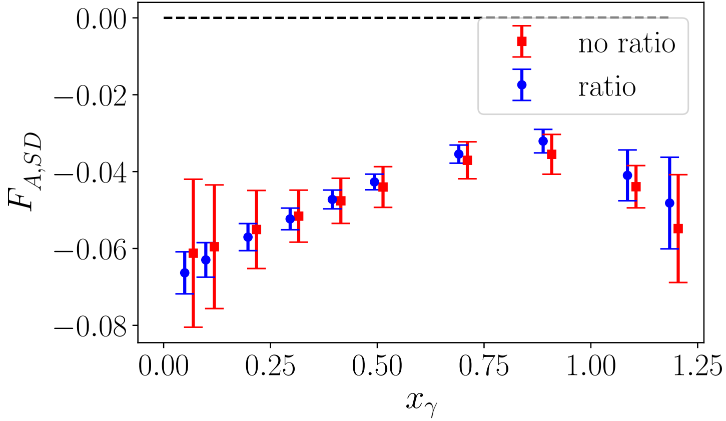

Averaging over $\pm\vec{p}_\gamma$

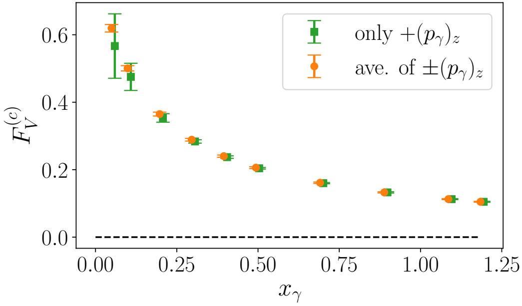

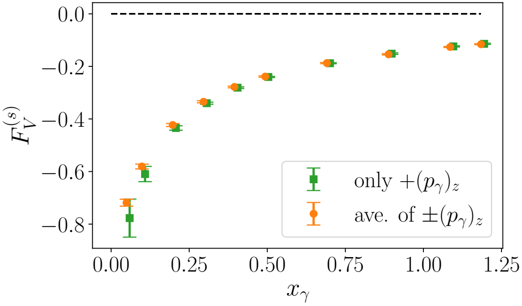

Outline for section 4

1. Introduction and Motivation
2. Extracting the hadronic tensor with Euclidean correlation functions
3. Methods study
4. $D_s \to \ell\nu_\ell\gamma$ preliminary form factor results

$D_s \to \ell\nu_\ell\gamma$ preliminary results

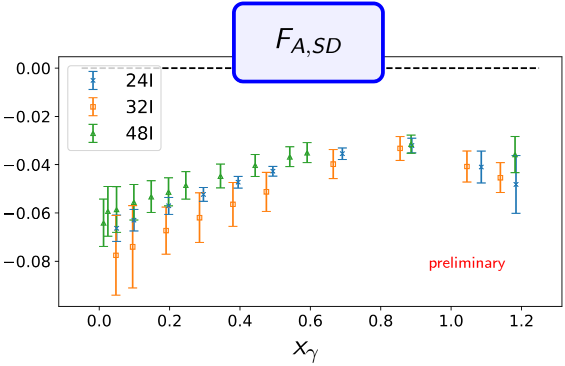

We are testing various fit functions to provide a parameterization of the form-factor lattice data

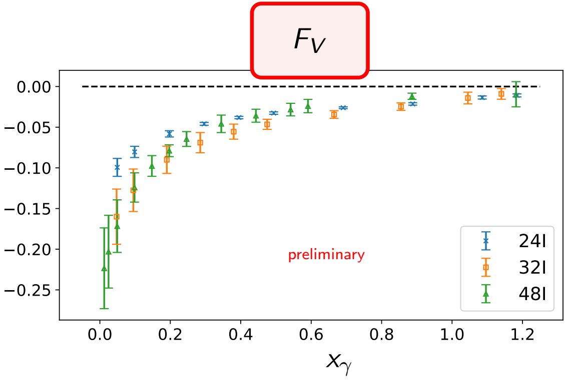

$D_s \to \ell\nu_\ell\gamma$ preliminary results

[1] [C. Donald, et. al, PRL 2014/arXiv:1312.5264]

[2] [Pullin, Zwicky, JHEP 2021/arXiv:2106.13617]

similar cancellations observed in $D_s D_s^* \gamma$ couplings, corresponding to pole residues in $D_s \to \gamma\ell\nu_\ell$ form factors [1],[2]

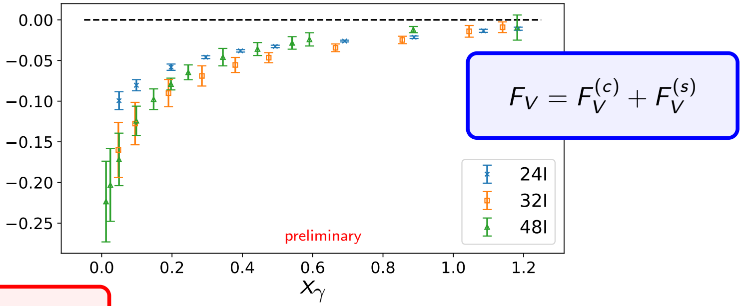

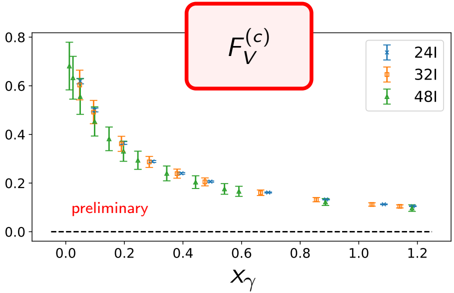

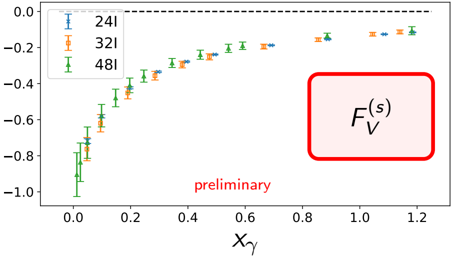

$D_s \to \ell\nu_\ell\gamma$ comparison

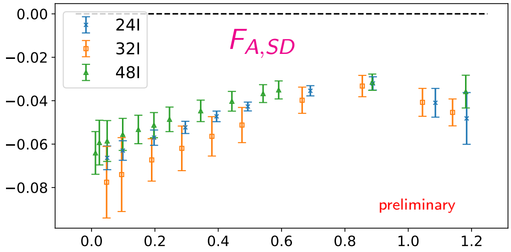

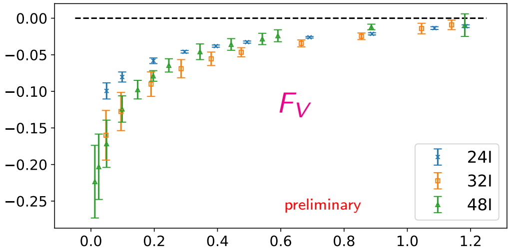

sign: different convention in FF decomp

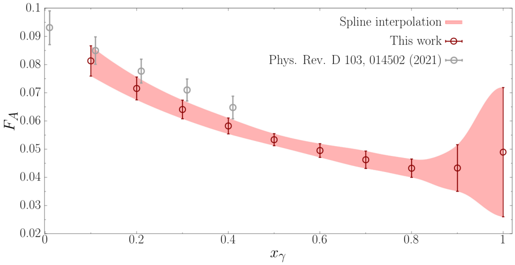

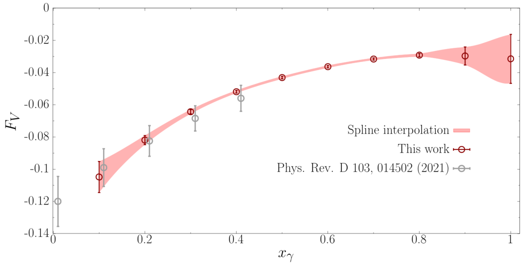

$D_s \to \ell \nu_\ell \gamma$ comparison

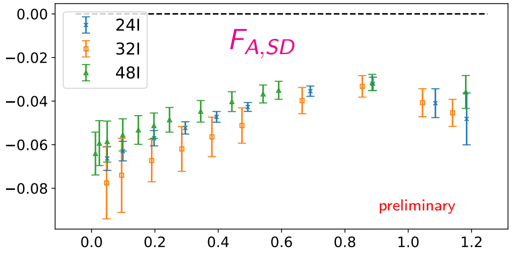

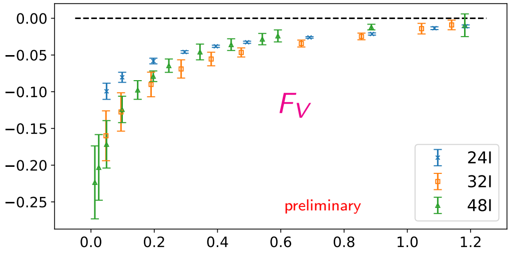

sign: different convention in FF decomp

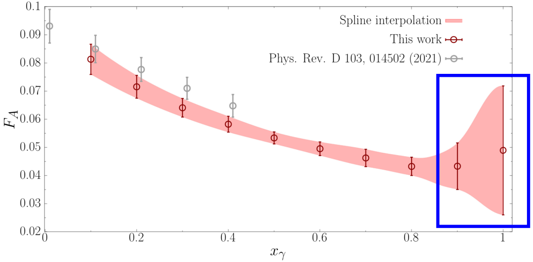

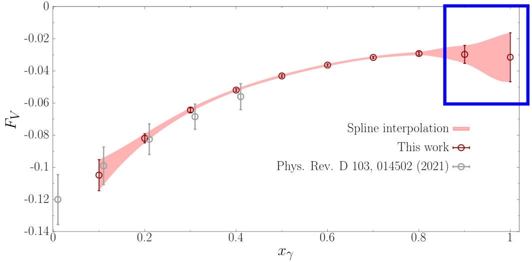

$D_s \to \ell \nu_\ell \gamma$ comparison

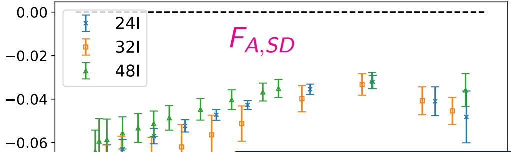

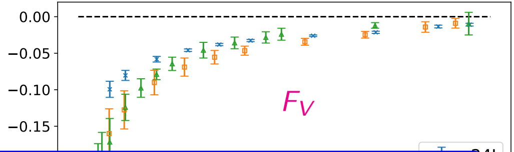

At large x_γ, signal to noise decays exponentially with T
(observed in [R. Frezzotti et. al, arXiv:2306.05904])
Can be tamed using 3d method

sign: different convent

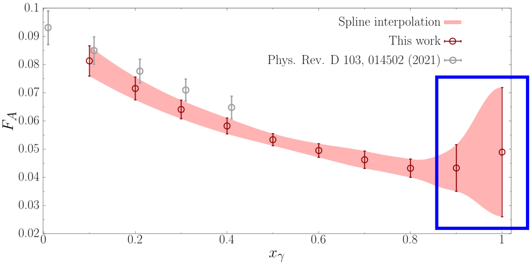

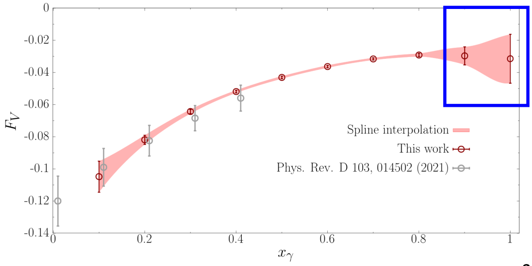

Future work

- Investigating different fit models to parameterize lattice form factors
- Improving statistics with new computing allocation from ACCESS
- Go to the B using new RBC-UKQCD $a^{-1} \approx 3.5$ GeV and 4.5 GeV lattices
- Have data for π, K, D, analyze this and compare our results to physical calculation in [Desiderio et. al, PRD 2021, arXiv:2006.05358] and experiment as was done in [Frezzotti et. al, PRD 2021, arXiv:2012.02120]

Summary

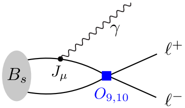

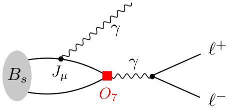

- Radiative leptonic decays are physically interesting at large and small photon momentum

Summary

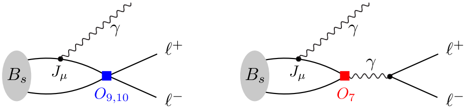

- Radiative leptonic decays are physically interesting at large and small photon momentum
- Two sources of systematic errors inherent in lattice QCD calc., need to take $T \to \infty$ and $t_H \to -\infty$

$$T_{\mu\nu} = \lim_{T\to\infty} \lim_{t_H\to-\infty} \frac{-2E_H e^{-E_H t_H}}{\langle H(\vec{p}_H)|\phi_H^\dagger|0\rangle} I_{\mu\nu}(T, t_H)$$

Summary

- Radiative leptonic decays are physically interesting at large and small photon momentum
- Two sources of systematic errors inherent in lattice QCD calc., need to take $T \to \infty$ and $t_H \to -\infty$
- Compared 3d sequential propagator and 4d sequential propagtors
  $\to$ found 3d method to offer good control over systematic uncertainties for cheapest cost

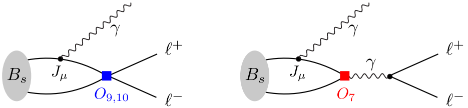

$$T_{\mu\nu} = \lim_{T\to\infty} \lim_{t_H\to-\infty} \frac{-2E_H e^{-E_H t_H}}{\langle H(\vec{p}_H)|\phi_H^\dagger|0\rangle} I_{\mu\nu}(T, t_H)$$

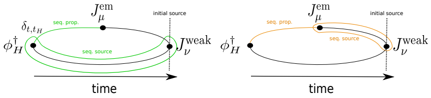

Summary

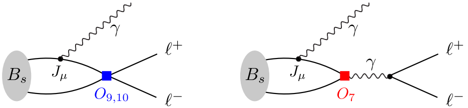

$$T_{\mu\nu} = \lim_{T\to\infty} \lim_{t_H\to-\infty} \frac{-2E_H e^{-E_H t_H}}{\langle H(\vec{p}_H)|\phi_H^\dagger|0\rangle} I_{\mu\nu}(T, t_H)$$

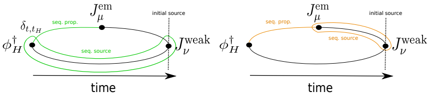

- Radiative leptonic decays are physically interesting at large and small photon momentum
- Two sources of systematic errors inherent in lattice QCD calc., need to take $T \to \infty$ and $t_H \to -\infty$
- Compared 3d sequential propagator and 4d sequential propagtors
  $\to$ found 3d method to offer good control over systematic uncertainties for cheapest cost
- Implemented number of improvements to 3d method

Summary

- Radiative leptonic decays are physically interesting at large and small photon momentum
- Two sources of systematic errors inherent in lattice QCD calc., need to take $T \to \infty$ and $t_H \to -\infty$
- Compared 3d sequential propagator and 4d sequential propagtors
  $\to$ found 3d method to offer good control over systematic uncertainties for cheapest cost
- Implemented number of improvements to 3d method
- Presented preliminary results for $D_s \to \gamma\ell\nu$ on three RBC/UKQCD ensembles using DWF for all flavors

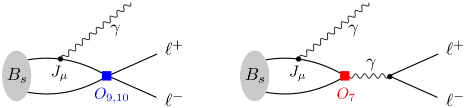

$$T_{\mu\nu} = \lim_{T\to\infty} \lim_{t_H\to-\infty} \frac{-2E_H e^{-E_H t_H}}{\langle H(\vec{p}_H)|\phi_H^\dagger|0\rangle} I_{\mu\nu}(T, t_H)$$

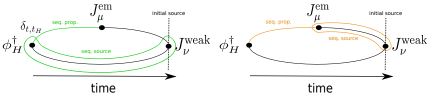

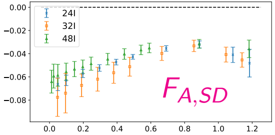

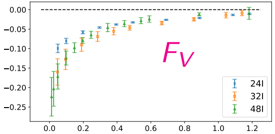

Main Take-Away Points

Main Take-Away Point 1: Radiative leptonic decays are interesting in the regions of small and large photon energies

Main Take-Away Point 2: We have developed methods to achieve high precision for small computational cost

for more details: D. Giusti, **CFK**, C. Lehner, S. Meinel, A. Soni, PRD 2023 / arXiv:[2302.01298]

Main Take-Away Point 3: Working on physical calculation of $D_s \to \gamma \ell \nu_\ell$, out soon

Backup slides

Time order visualization

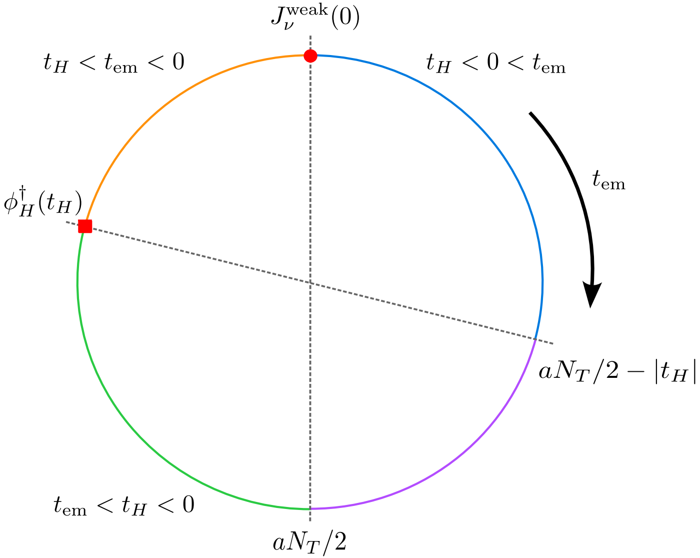

Minkowski spectral decomposition of $T_{\mu\nu}$

Time ordering $t_{em} < 0$:

$$\widehat{1} = |0\rangle\langle 0| + \sum_n \int \frac{d^3p}{(2\pi)^3} \frac{1}{2E_n(\vec{p})} |n(\vec{p})\rangle\langle n(\vec{p})|$$

$$\begin{aligned} T^{<}_{\mu\nu} &= -i \int_{-\infty(1-i\epsilon)}^{0} dt_{em} \int d^3x \; e^{ip_\gamma \cdot x} \langle 0| J^{weak}_\nu(0) \widehat{1} J^{em}_\mu(x) |B^-(\vec{p}_B)\rangle \\ &= -\sum_n \frac{1}{2E_{n,\vec{p}_B-\vec{p}_\gamma}} \frac{1}{E_\gamma + E_{n,\vec{p}_B-\vec{p}_\gamma} - E_{B,\vec{p}_B} - i\epsilon} \\ &\qquad \times \langle 0| J^{weak}_\nu(0) |n(\vec{p}_B - \vec{p}_\gamma)\rangle\langle n(\vec{p}_B - \vec{p}_\gamma)| J^{em}_\mu(0) |B(\vec{p}_B)\rangle \end{aligned}$$

(In infinite volume, the sum over n includes an integral over the continuous spectrum of multi-particle states.)

Euclidean spectral decomposition of $I_{\mu\nu}$

Time ordering $t_{em} < 0$: (for large negative t_B)

$$
\begin{aligned}
I^{<}_{\mu\nu}(t_B, T) &= \int_{-T}^{0} dt_{em}\; e^{E_\gamma t} C_{3,\mu\nu}(t_{em}, t_B) \\
&= \langle B(\vec{p}_B)|\phi_B^\dagger(0)|0\rangle \frac{1}{2E_{B,\vec{p}_B}} e^{E_B t_B} \\
&\times \sum_n \frac{1}{2E_{n,\vec{p}_B-\vec{p}_\gamma}} \frac{\langle 0|J_\nu^{weak}(0)|n(\vec{p}_B-\vec{p}_\gamma)\rangle\langle n(\vec{p}_B-\vec{p}_\gamma)|J_\mu^{em}(0)|B(\vec{p}_B)\rangle}{E_\gamma + E_{n,\vec{p}_B-\vec{p}_\gamma} - E_{B,\vec{p}_B}} \\
&\times \left[1 - e^{-(E_\gamma + E_{n,\vec{p}_B-\vec{p}_\gamma} - E_{B,\vec{p}_B})T}\right]
\end{aligned}
$$

(* all times are now Euclidean)

Require $E_\gamma + E_{n,\vec{p}_B-\vec{p}_\gamma} - E_{B,\vec{p}_B} > 0$ to get rid of unwanted exponential

States $|n(\vec{p}_B - \vec{p}_\gamma)\rangle$ has same flavor quantum numbers as B meson

$\rightarrow E_{n,\mathbf{p}_B-\mathbf{p}_\gamma} \geq E_{B,\mathbf{p}_B-\mathbf{p}_\gamma} = \sqrt{m_B^2 + (\mathbf{p}_B - \mathbf{p}_\gamma)^2}$

For $\mathbf{p}_\gamma \neq 0$, $|\mathbf{p}_\gamma| + \sqrt{m_n^2 + (\mathbf{p}_B - \mathbf{p}_\gamma)^2} > \sqrt{m_B^2 + \mathbf{p}_B}$ is automatically satisfied

Comparison to experiment and lattice: [PRD 2021/arXiv:2012.02120]

Depends on $F^{\pm}(x_\gamma) = F_V(x_\gamma) \pm F_{A,SD}(x_\gamma)$, at $\mathcal{O}(\alpha_{\text{em}})$, three pieces

- Point-like (pt): universal, does not probe internal structure of meson
- Structure-dependent: $\text{SD} \sim \text{SD}^+((F^+)^2) + \text{SD}^-((F^-)^2)$
- Interference between (pt) and (SD): $\text{INT} \sim \text{INT}^-(F^+) + \text{INT}^-(F^-)$

KLOE experiment

- $K \to e\nu_e\gamma$: perform cuts so senstive to mainly $\text{SD}^+ \implies (F^+)^2)$ consistent
- $K \to \mu\nu_\mu\gamma$: perform cuts so senstive to

E787 experiment:

- $K \to \mu\nu_\mu\gamma$: perform cuts so senstive to mainly $\text{SD}^+ \implies (F^+)^2)$, slight dependence on $\text{SD}^- + \text{INT}^-$ at small x_γ
- Tension between prediction for $F(x_\gamma)^+$ between KLOE and E787

Rough summary

Let $F^{\pm}(x_\gamma) = F_V(x_\gamma) \pm F_{A,SD}(x_\gamma)$, then

Piece	QCD FF
PT	none
SD$^+$	$(F^+)^2$
SD$^-$	$(F^-)^2$
INT$^+$	F^+
INT$^-$	F^-

Experiment	Process	Sensitive to	Theory vs Exp.
KLOE	$K \to e\nu_e\gamma$	SD$^+$	Agree
E787	$K \to \mu\nu_\mu\gamma$	SD$^+$, SD$^-$ + INT$^-$	Tension
ISTRA+	$K \to \mu\nu_\mu\gamma$	INT$^-$	Tension
OKA	$K \to \mu\nu_\mu\gamma$	INT$^-$	Tension
PIBETA	$\pi \to e\nu_e\gamma$	SD$^+$	Tension

Fit form: 4d method

Use fit ranges where data has plateaued in t_H, i.e. $t_H \to -\infty$

Include terms to fit
(1) unwanted exponential from first intermediate state

Limitation of 4d method $\to$ cannot resolve the two time orderings
$\to$ Fit sum of both time orderings $F_V(T, t_H) = F_V^{<}(T, t_H) + F_V^{>}(T, t_H)$

$$F(t_H, T) = F + B_F^{<} \underbrace{e^{-(E_\gamma - E_H + E^{<})T}}_{t_{em}<0} + B_F^{>} \underbrace{e^{(E_\gamma - E^{>})T}}_{t_{em}>0}$$

■ fit parameters

Only have three values of T, fitting multiple exponentials not possible
$\to$ Use broad Gaussian prior on $E^{>}$ exclude unphysical values

Comparison of 4d and 4d$^{>,<}$

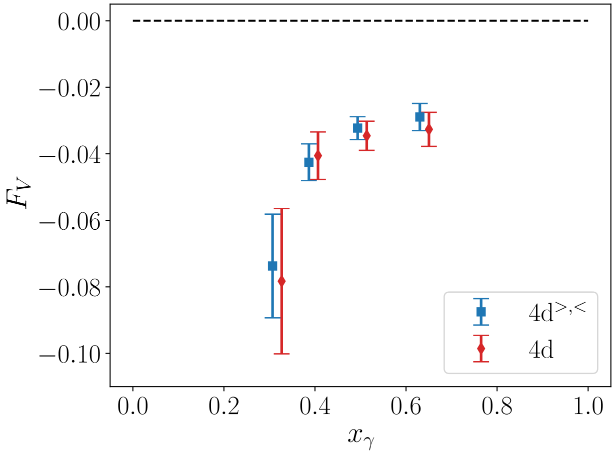

$$x_\gamma = 2E_\gamma^{(0)}/m_{D_s}$$

$$0 \le x_\gamma \le 1 - \frac{m_\ell^2}{m_{D_s}^2}$$

Summary:

- Cost 4d$^{>,<}$ method roughly twice 4d method
- 4d$^{>,<}$ resolves time orders, allows better control over $T \to \infty$ limit
- 4d$^{>,<}$ method smaller uncertainty than 4d method

Infinite volume approximation

For point-sources use translational invariance to fix em/weak operator at origin
$\rightarrow$ use "infinite-volume approximation" to generate data at arbitrary photon momenta
$\rightarrow$ only exponentially small FVEs introduced

Infinite volume approximation

For point-sources use translational invariance to fix em/weak operator at origin
$\rightarrow$ use "infinite-volume approximation" to generate data at arbitrary photon momenta
$\rightarrow$ only exponentially small FVEs introduced

Strategy:

- Work in rest frame of D_s meson
- Calculate correlation function for arbitrary values of photon momentum
- Propagator solves per config
  $\rightarrow 2(1 + N_{t_H})$

Infinite volume approximation

For point-sources use translational invariance to fix em/weak operator at origin
$\rightarrow$ use "infinite-volume approximation" to generate data at arbitrary photon momenta
$\rightarrow$ only exponentially small FVEs introduced

Strategy:

- Work in rest frame of D_s meson
- Calculate correlation function for arbitrary values of photon momentum
- Propagator solves per config
  $\rightarrow 2(1 + N_{t_H})$

Photon momenta for 24I ensemble:

$$p_{\gamma,z} = 2\pi/L \times \{0.1, 0.2, 0.4, 0.6, 0.8, 1.0, 1.4, 1.8, 2.2, 2.4\}$$

$$C_{3,\mu\nu}(t_{em}, t_H) = \int d^3x \int d^3y \; e^{-i\vec{p}_\gamma \cdot \vec{x}} \langle J_\mu^{\text{em}}(t_{em}, \vec{x}) J_\nu^{\text{weak}}(0) \phi_H^\dagger(t_H, \vec{y}) \rangle$$

Infinite volume approximation

We assume there exist $c, d, \Lambda, \Lambda' \in \mathbb{R}^+$ and $L_0 \in \mathbb{N}$ for which

$$\tilde{C}^L(q) \equiv \sum_{x=-L/2}^{L/2-1} C^L(x) e^{iqx}$$

for all x with $-L/2 \leq x \leq L/2$ and $L \geq L_0$ and

$$|C^\infty(x)| \leq d e^{-\Lambda' |x|}$$

for all x with $|x| > L/2$. We now define

$$|C^\infty(x) - C^L(x)| \leq c e^{-\Lambda L} \qquad \text{and} \qquad \tilde{C}^\infty(q) \equiv \sum_{x=-\infty}^{\infty} C^\infty(x) e^{iqx} .$$

Under the above assumptions, it then follows that there is a $\tilde{c} \in \mathbb{R}^+$ for which

$$|\tilde{C}^\infty(q) - \tilde{C}^L(q)| \leq \tilde{c} e^{-\Lambda_0 L}$$

for all $q \in [-\pi, \pi]$ and all $L \geq L_0$, with $\Lambda_0 \equiv \min(\Lambda, \Lambda'/2)$.

Fits to 3d data for F_V with improved methods

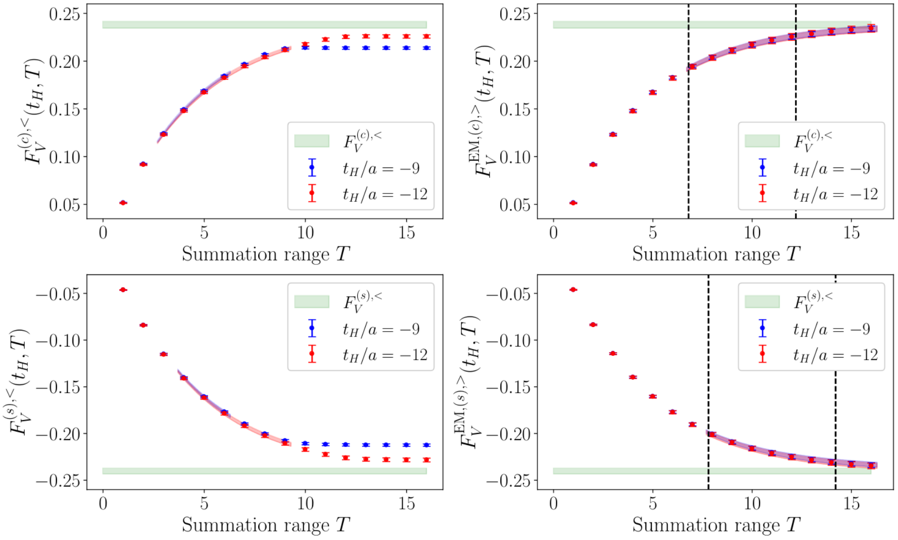

Fits to 3d data for $F_{A,SD}$ with improved methods

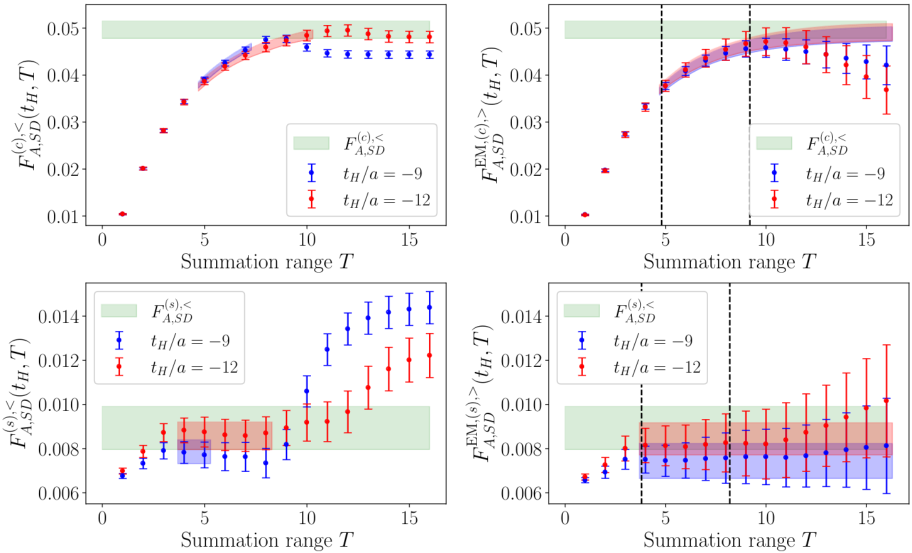

Simulation parameters

Physical calculation for π, K, D, D_s [Desiderio, Frezzotti, Garofalo, Giusti, Hansen, Lubicz, Martinelli, Sachrajda, Sanfilippo, Simula, Tantalo, PRD 2021, arXiv:2006.05358]

- 3 ETMC gauge ensembles with $N_f = 2+1+1$
- twisted mass fermions in sea?
- 3 lattice spacings $a \in \{0.089, 0.082, 0.062\}$ fm
- Lightest
- twisted boundary conditions to assign arbitrary $p_\gamma, p_{\text{Meson}}$

Physical calculation for $D_s \to \gamma \ell \nu_\ell$ for full kinematic range of E_γ [Frezzotti, Gagliardi, Lubicz, Martinelli, Mazzetti, Sachrajda, Sanfilippo, Simula, Tantalo, PRD 2021, arXiv:2306.05904]

- 4 ETMC gauge ensembles with $N_f = 2+1+1$
- twisted mass fermions
- 4 lattice spacings $a \in [0.058, 0.09]$ fm
- physical pion mass
- twisted boundary conditions to assign arbitrary p_γ, p_{D_s}
- Osterwalder-Seiler fermions